expressed in primary ATL cells. We therefore first examined the mRNA expression of the AP-1 family members in primary ATL cells freshly isolated from patients in comparison with normal CD4+ T cells in resting, activated and Th1/Th2-polarized conditions (Figure 2a). As reported previously (Yoshie *et al*., 2002; Nagakubo *et al*., 2007), primary ATL cells consistently expressed CCR4 at levels much higher than various normal CD4+ T-cell populations, including Th2-polarized cultured T cells. Furthermore, primary ATL cells consistently expressed Fra-2 in sharp contrast to various normal CD4+ T-cell populations that were essentially negative for Fra-2 expression. Similar to various normal CD4+ T-cell populations, primary ATL

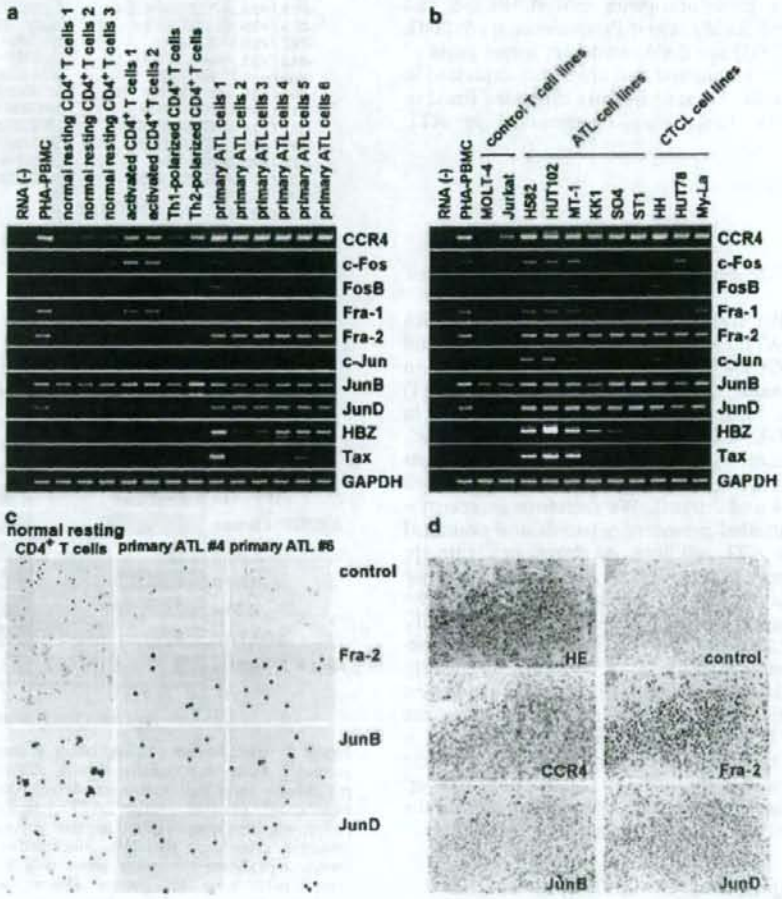

Figure 2 Constitutive expression of Fra-2, JunB and JunD in adult T-cell leukemia (ATL). (**a**) Reverse transcription (RT)–PCR analysis for the expression of the AP-1 family in normal T cells and primary ATL cells. Normal resting CD4+ T cells (purity, >96%) from healthy donors ($n=3$), activated CD4+ T cells from normal donors ($n=2$), Th1-polarized cultured CD4+ T cells, Th2-polarized cultured CD4+ T cells and freshly isolated primary ATL cells (>90% leukemic cells) from patients ($n=6$) were examined as indicated. Normal peripheral blood mononuclear cells treated with phytohemagglutinin (PHA-PBMC) served as a positive control. GAPDH served as a loading control. The representative results from at least two separate experiments are shown. (**b**) RT–PCR analysis for the expression of the AP-1 family in human T-cell lines. Two control human T-cell lines, six ATL cell lines and three CTCL cell lines were examined as indicated. PHA-PBMC served as a positive control. GAPDH served as a loading control. The representative results from two separate experiments are shown. (**c**) Immunocytochemical staining for Fra-2, JunB and JunD in normal CD4+ T cells and primary ATL cells. Normal CD4+ T cells from healthy donors (purity, >96%) and primary ATL cells (leukemic cells, >90%) from two patients were stained with anti-Fra-2, anti-JunB or anti-JunD. Normal rabbit IgG was used as the negative control (control). The representative results from two separate experiments are shown. Original magnification: ×400. (**d**) Immunohistochemical staining of CCR4, Fra-2, JunB and JunD in ATL skin lesions. Tissue sections from ATL skin lesions ($n=6$) were stained with anti-CCR4, anti-Fra-2, anti-JunB or anti-JunD. Mouse IgG_1 and normal rabbit IgG were used as the negative controls (control). Tissue sections were counterstained using Gill's hematoxylin. The representative results from a single donor are shown. Original magnification: ×400.

cells also constitutively expressed JunD and JunB even though JunD expression appeared to be upregulated in primary ATL cells. Other members of the AP-1 family were mostly negative in primary ATL cells, while activated normal CD4+ T cells expressed c-Fos, Fra-1 and c-Jun at high levels. There was no correlation in expression between Fra-2 and the virally encoded HTLV-1 basic leucine zipper factor HBZ or Tax in primary ATL cells. We also confirmed that Fra-2 is not inducible by Tax using JPX-9, a subline of Jurkat carrying the HTLV-1 Tax gene under the control of the metallothionein gene promoter (Nagata *et al.*, 1989; data not shown). Thus, the constitutive expression of Fra-2 is highly unique for primary ATL cells.

We also examined expression of the same set of genes in various human T-cell lines. As shown in Figure 2b, compared to control T-cell lines, ATL cell lines consistently expressed CCR4 and Fra-2 at high levels. ATL cell lines also expressed JunB and JunD at high levels. HTLV-1 Tax has been shown to induce various AP-1 family members (Nagata *et al.*, 1989; Iwai *et al.*, 2001), which may be involved in HTLV-1 gene expression and cell proliferation (Jeang *et al.*, 1991). Consistently, ATL cell lines expressing Tax (H582, HUT102 and MT-1) also expressed other AP-1 family members at low levels. Cutaneous T-cell lymphomas (CTCLs) are a subset of HTLV-1-negative T-cell lymphomas resembling ATL and known to be frequently positive for CCR4 (Kim *et al.*, 2005). CTCL cell lines were also found to strongly express CCR4, Fra-2, JunB and JunD. Thus, the constitutive expressions of Fra-2, JunB and JunD were shared by CCR4-expressing ATL and CTCL cell lines.

We also examined the Fra-2, JunB and JunD protein expression in freshly isolated primary ATL cells and normal resting CD4+ T cells. As shown in Figure 2c, primary ATL cells were indeed stained strongly positive for Fra-2, while normal CD4+ T cells were totally negative for Fra-2. Primary ATL cells were also strongly positive for JunB and JunD, while normal CD4+ T cells were variably positive for JunB and JunD at the single cell level. These results were highly consistent with the results from reverse transcription (RT)–PCR; Figure 2a). We also confirmed the CCR4, Fra-2, JunB and JunD protein expression in skin-infiltrating ATL cells (Figure 2d).

Activation of the CCR4 promoter by Fra-2/JunB and Fra-2/JunD heterodimers

AP-1 is known to function as a heterodimer of a member of the Fos family (c-Fos, FosB, Fra-1 and Fra-2) and a member of the Jun family (c-Jun, JunB and JunD) or a homodimer of the Jun family (Shaulian and Karin, 2002; Eferl and Wagner, 2003). We, therefore, next examined the activation of the CCR4 promoter by individual AP-1 family members singly or in combination. As recipients, we used two T-cell lines, namely, MOLT-4 and Jurkat. The expression levels of AP-1 members, including Fra-2, JunB and JunD, were very low in these cell lines (Figure 2b). As shown in Figure 3a, only Fra-2/JunB or Fra-2/JunD potently activated the CCR4 promoter in both cell lines. We confirmed that other members of the AP-1 family (c-Fos, FosB, Fra-1 and c-Jun) were transcriptionally active by using a synthetic promoter containing two tandem AP-1 consensus-binding sites (pGL3-2xAP-1; Figure 3b). Thus, among the AP-1 family members, only the Fra-2/JunB and Fra-2/JunD heterodimers are uniquely capable of activating the CCR4 promoter. This is highly consistent with their constitutive expression in primary ATL cells (Figure 2a).

Recently, the mRNA of HTLV-1 HBZ has been shown to be expressed in primary ATL cells (Satou *et al.*, 2006). We indeed observed the expression of HBZ in some primary ATL samples (Figure 2a). HBZ has been shown to activate JunB homodimer- or JunD homodimer-dependent transcription (Basbous *et al.*, 2003; Thebault *et al.*, 2004). Therefore, we also examined the effects of HBZ as well as Tax on the CCR4 promoter in MOLT-4 and Jurkat cells. As shown in Figure 3c, HBZ alone or in combination with Fra-2, JunB, JunD, Fra-2/JunB or Fra-2/JunD showed no effect on the activation of the CCR4 promoter. Similarly, Tax had no significant effect on the CCR4 promoter either alone or in combination with Fra-2, JunB, JunD, Fra-2/JunB or Fra-2/JunD. Thus, HTLV-1 encoded HBZ or Tax neither activates the CCR4 promoter nor affects its activation by Fra-2/JunB or Fra-2/JunD.

We have also confirmed that GATA-3 is constitutively expressed in primary ATL cells and activates the CCR4 promoter (data not shown). In normal CD4+ T cells, GATA-3 may be responsible for the selective expression of CCR4 in Th2 cells (Imai *et al.*, 1999; Rengarajan *et al.*, 2000).

Specific binding of Fra-2, JunB and JunD to the AP-1 site in the CCR4 promoter

We next examined the specific binding of AP-1 family members to the AP-1 site in the CCR4 promoter using the NoShift transcription factor assay, an enzyme-linked immunosorbent assay (ELISA)-like colorimetric assay that is an alternative to the electrophoretic mobility shift assay. As shown in Figure 4a, when the nuclear extracts of two control T-cell lines (MOLT-4 and Jurkat) were used, the specific binding of any AP-1 family members to the AP-1 site of the CCR4 promoter was hardly observed. On the other hand, when the nuclear extracts of two ATL cell lines (HUT102 and ST1) were used, we detected a high level of specific binding of Fra-2, JunB and JunD to the AP-1 site. These results are highly consistent with the results from RT–PCR analyses (Figure 2b) and the luciferase reporter assays (Figure 3a).

By using the chromatin immunoprecipitation (ChIP) assay, we further examined the binding of Fra-2, JunB and JunD to the AP-1 site of the CCR4 promoter *in vivo*. As shown in Figure 4b, we detected specific binding of Fra-2, JunB and JunD to the AP-1 site of the endogenous CCR4 promoter in primary ATL cells but not in normal CD4+ T cells. These results further

support the hypothesis that the CCR4 gene is a direct target gene of Fra-2/JunB and Fra-2/JunD heterodimers in primary ATL cells.

Effects of Fra-2, JunB and JunD small interfering RNAs on CCR4 expression and cell proliferation

To examine the role of Fra-2, JunB and JunD in CCR4 expression and cell proliferation in ATL cells, we next employed the small interfering RNA (siRNA) knockdown technique. As shown in Figure 5a, Fra-2 siRNA, JunB siRNA and JunD siRNA specifically reduced Fra-2 mRNA, JunB mRNA and JunD mRNA, respectively, in two ATL cell lines. On the other hand, control siRNA showed no such effect. Under these conditions, we examined the effects of these siRNAs on CCR4 expression and cell growth. As shown in Figure 5b, Fra-2 siRNA and JunD siRNA reduced CCR4 expression by approximately 50% in both cell lines, whereas JunB siRNA had hardly any inhibitory effect and control siRNA showed no inhibitory effect. Furthermore, as shown in Figure 5c, Fra-2 siRNA and JunD siRNA significantly reduced cell proliferation in both cell lines, whereas JunB siRNA or control siRNA did not. None of the siRNAs affected the growth of the control T-cell lines MOLT-4 and Jurkat. We also compared the effects of single and double knockdown of Fra-2 and JunD on cell growth in two ATL cell lines (Figure 5d). Compared to the effect of single knockdown of Fra-2 or JunD, no additive effect was observed by double knockdown of Fra-2 and JunD in both cell lines. These results may be consistent with the notion that Fra-2 and JunD promote growth in ATL cell lines by functioning as a heterodimer.

To further demonstrate the growth-promoting effects of Fra-2 and JunD, we performed stable transfection of Fra-2 and JunD in the control T-cell line Jurkat. As shown in Figure 5e, Jurkat cells overexpressing Fra-2 or JunD (see inset) indeed showed enhanced growth compared to those transfected with the vector alone. We were, however, unable to isolate Fra-2/JunD double transfectants in Jurkat, probably because of some adverse effects on Jurkat cells by the overexpression of both Fra-2 and JunD.

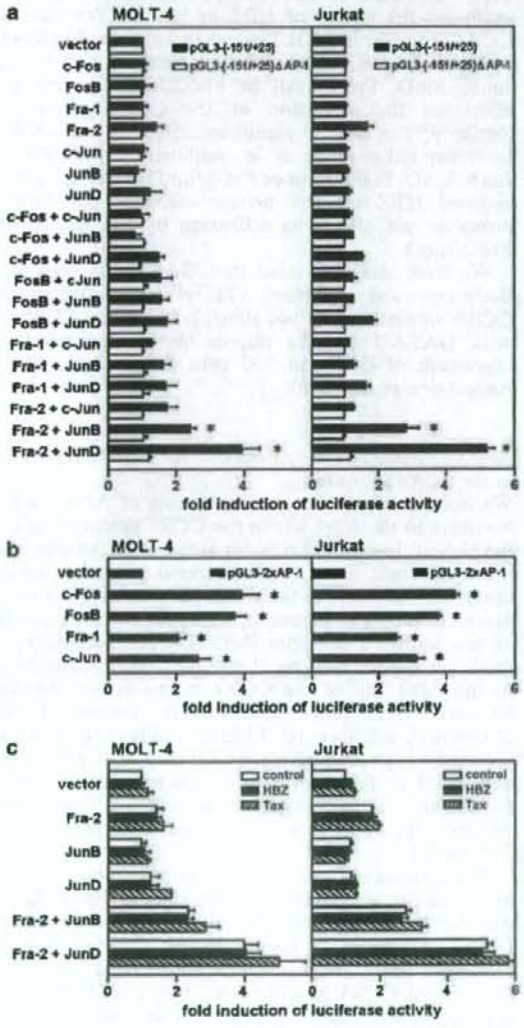

Figure 3 Transactivation of the CCR4 promoter by Fra-2/JunD and Fra-2/JunB. (**a**) Transactivation of the CCR4 promoter with or without the AP-1 site. MOLT-4 and Jurkat cells were cotransfected with pSV-β-galactosidase and pGL3-CCR4 (−151/+25) or pGL3-CCR4 (−151/+25)ΔAP-1 and an expression vector for c-Fos, FosB, Fra-1, Fra-2, c-Jun, JunB, JunD or a control vector as indicated. After 24–27 h, luciferase assays were performed in triplicate. Promoter activation was expressed as the fold induction of luciferase activity in cells transfected with an indicated AP-1 expression vector versus cells transfected with the vector alone. Transfection efficiency was normalized by β-galactosidase activity. Each bar represents the mean ± s.e.m. from three separate experiments. $^*P<0.05$. (**b**) Transactivation of a synthetic promoter with two copies of the consensus AP-1 site. MOLT-4 and Jurkat cells were cotransfected with pSV-β-galactosidase and pGL3-2xAP-1 and an expression vector for c-Fos, FosB, Fra-1, c-Jun or the vector alone as indicated. Promoter activation was expressed as the fold induction of luciferase activity in cells transfected with an indicated expression vector versus cells transfected with a control vector. After 24–27 h, luciferase assays were performed in triplicate. Transfection efficiency was normalized by β-galactosidase activity. Each bar represents the mean ± s.e.m. from three separate experiments. $^*P<0.05$. (**c**) Effect of HBZ or Tax on the activation of the CCR4 promoter. MOLT-4 and Jurkat cells were cotransfected with pSV-β-galactosidase and the pGL3-basic vector or pGL3-CCR4 (−151/+25) and an expression vector for Fra-2, JunB, JunD or a control vector and an expression vector for HBZ, Tax or a control vector as indicated. After 24–27 h, luciferase assays were performed in triplicate. Promoter activation was expressed as the fold induction of luciferase activity in cells transfected with an indicated expression vector versus cells transfected with a control vector. Transfection efficiency was normalized by β-galactosidase activity. Each bar represents the mean ± s.e.m. from three separate experiments.

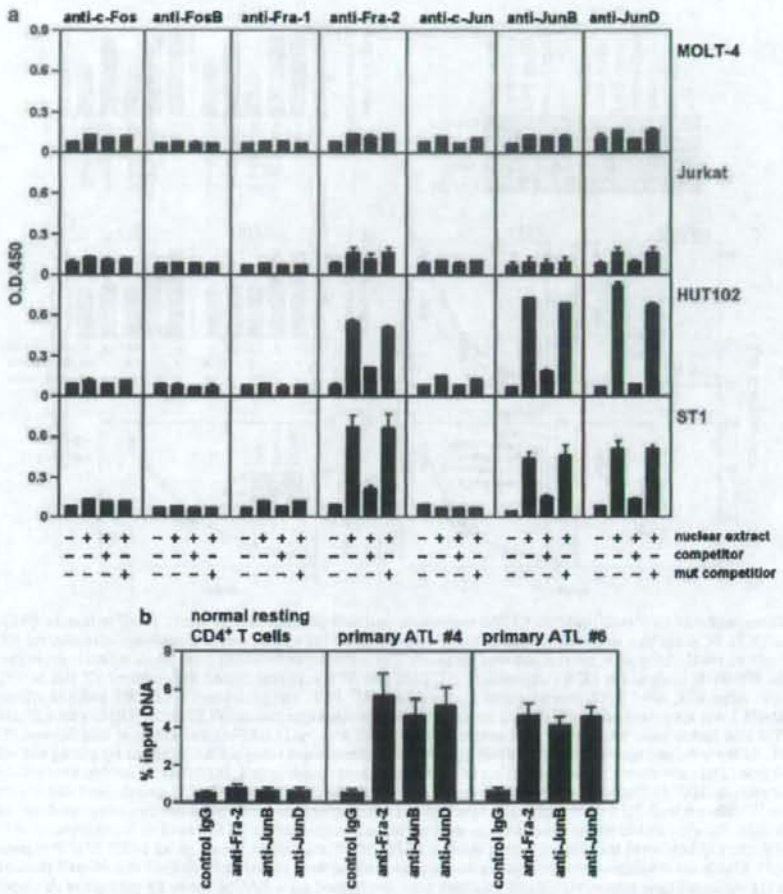

Figure 4 Specific binding of Fra-2, JunB and JunD to the AP-1 site in the CCR4 promoter. (a) NoShift assay. Nuclear extracts were prepared from two control T-cell lines (MOLT-4 and Jurkat) and two adult T-cell leukemia (ATL) cell lines (HUT102 and ST1). Nuclear proteins that bound to the biotinylated AP-1 site oligonucleotide (TGGGAAATGACTAAGAATCAT) were captured on an avidin-coated plate and detected by anti-c-Fos, anti-FosB, anti-Fra-1, anti-Fra-2, anti-c-Jun, anti-JunB or anti-JunD, as indicated. Specificity was determined by adding unlabeled probe (competitor; TGGGAAATGACTAAGAATCAT) or mutant probe (mut competitor; TGGGAAATGTCAAAGAATCAT; differences underlined). Each bar represents the mean ± s.e.m. from three separate experiments. (b) Chromatin immunoprecipitation (ChIP) assay. Chromatins from normal CD4+ T cells from healthy donors (purity, >96%) and primary ATL cells from two patients (leukemic cells, >90%) were immunoprecipitated with anti-Fra-2, anti-JunD or control IgG. The amounts of precipitated DNA relative to total input DNA were quantified by real-time PCR for the CCR4 promoter region containing the AP-1 site. Each bar represents the mean ± s.e.m. from three separate experiments.

Identification of downstream target genes of the Fra-2/JunD heterodimer in ATL cells

To identify the target genes of Fra-2 in ATL cells, we compared the gene expression profiles of ATL-derived ST1 cells transfected with Fra-2 siRNA or control siRNA using the Affymetrix high-density oligonucleotide microarray. As summarized in Figure 6a, at least 49 genes were downregulated more than threefold by Fra-2 siRNA. The classification of these genes according to their biological functions shows that Fra-2 promotes the expression of genes involved in signal transduction (10 genes), protein biosynthesis and modification (8 genes) and transcription (6 genes); it also stimulates the expression of 10 genes of unknown function. Most notably, the list includes the proto-oncogenes c-Myb, BCL-6 and MDM2 (Oh and Reddy, 1999; Pasqualucci *et al*., 2003; Vargas *et al*., 2003). As shown in Figure 6b, RT–PCR analysis verified that not only Fra-2 siRNA but also JunD siRNA downregulated these proto-oncogenes in two ATL cell lines. Therefore, c-Myb, BCL-6 and MDM2 are the downstream target genes of the Fra-2/JunD heterodimer in both cell lines. This prompted us to examine the expression of c-Myb, BCL-6 and MDM2 in freshly isolated primary ATL cells by

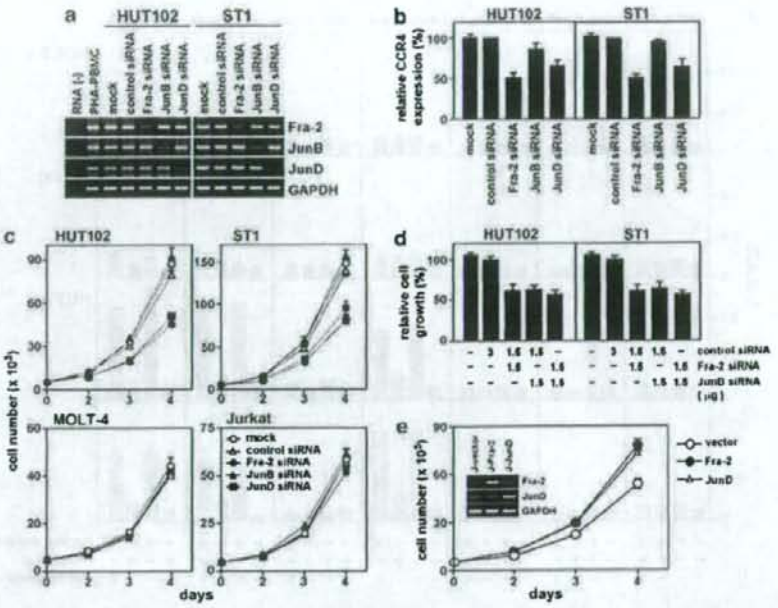

Figure 5 Dominant role of Fra-2/JunD in CCR4 expression and cell proliferation in adult T-cell leukemia (ATL). (a) Reverse transcription (RT)–PCR analysis to determine the effect of siRNAs. HUT102 and ST1 were transfected with control siRNA or siRNA for Fra-2, JunB or JunD. After 48 h, total RNA was prepared. The representative results from three separate experiments are shown. (b) Real-time RT–PCR analysis for CCR4 expression. HUT102 and ST1 were transfected with control siRNA or siRNA for Fra-2, JunB or JunD. After 48 h, total RNA was prepared and real-time RT–PCR was performed for CCR4 and 18S ribosomal RNA (an internal control). Data are presented as the mean ± s.e.m. of three separate experiments. (c) Effect of siRNAs on cell growth. HUT102, ST1, MOLT-4 and Jurkat were transfected with control, Fra-2, JunB and JunD siRNAs and cultured in a 96-well plate at 0.5×10^4 cells per well. At the indicated time points, viable cell numbers were determined using a FACSCalibur by gating out cells stained with propidium iodide. Data are shown as the mean ± s.e.m. of three separate experiments. (d) Effect of double knockdown of Fra-2 and JunD on cell growth. HUT102 and ST1 were transfected with control, Fra-2 and JunD siRNAs as indicated and cultured in a 96-well plate at 0.5×10^4 cells per well. At 4 days, viable cell numbers were determined on a FACSCalibur by gating out dead cells stained with propidium iodide. Data are shown as the mean ± s.e.m. of three separate experiments. (e) Effect of stable expression of Fra-2 and JunD on cell growth. Jurkat cells were transfected with a control IRES-EGFP expression vector or an IRES-EGFP expression vector for Fra-2 or JunD. Stable transfectants expressing green fluorescence protein were sorted and cultured in a 96-well plate at 0.5×10^4 cells per well. At the indicated time points, viable cell numbers were determined on a FACSCalibur by gating out dead cells stained with propidium iodide. Data are shown as the mean ± s.e.m. of three separate experiments.

RT–PCR. As shown in Figure 6c, we indeed detected the constitutive expression of c-Myb, BCL-6 and MDM2 at high levels in primary ATL cells. In sharp contrast, normal resting $CD4^+$ T cells hardly expressed these proto-oncogenes.

Discussion

The AP-1 transcription factors function as homodimers or heterodimers formed by Jun (c-Jun, JunB and JunD), Fos (c-Fos, FosB, Fra-1 and Fra-2) and the ATF family proteins (Shaulian and Karin, 2002; Eferl and Wagner, 2003). Most of them are rapidly and transiently induced by extracellular stimuli that trigger the activation of the Janus kinase (JNK), extracellular signal regulated protein kinases 1 and 2 (ERK1/2) or p38 mitogen-activated protein (MAP) kinase pathways (Shaulian and Karin, 2002; Eferl and Wagner, 2003). The AP-1 family is known to be involved in cellular proliferation, oncogenesis and even tumor suppression, depending on the combination of AP-1 proteins and the cellular context (Shaulian and Karin, 2002; Eferl and Wagner, 2003). Previously, by using the AP-1 site of the IL-8 promoter, Mori *et al.* demonstrated a strong Tax-independent expression of JunD in primary ATL cells (Mori *et al.*, 2000). In the present study, we have shown that Fra-2 is constitutively expressed at high levels in primary ATL cells (Figure 2a). Furthermore, except for JunB and JunD, other members of the AP-1 family are mostly negative in primary ATL cells (Figure 2a). Therefore, as demonstrated in the present study, the Fra-2/JunD and Fra-2/JunB heterodimers may be the major AP-1 factors constitutively active in primary ATL cells.

It has been shown that HTLV-1 Tax induces the expression of various AP-1 family members such as c-Fos, Fra-1, c-Jun and JunD (Nagata *et al.*, 1989; Iwai *et al.*, 2001). We indeed observed the expression of

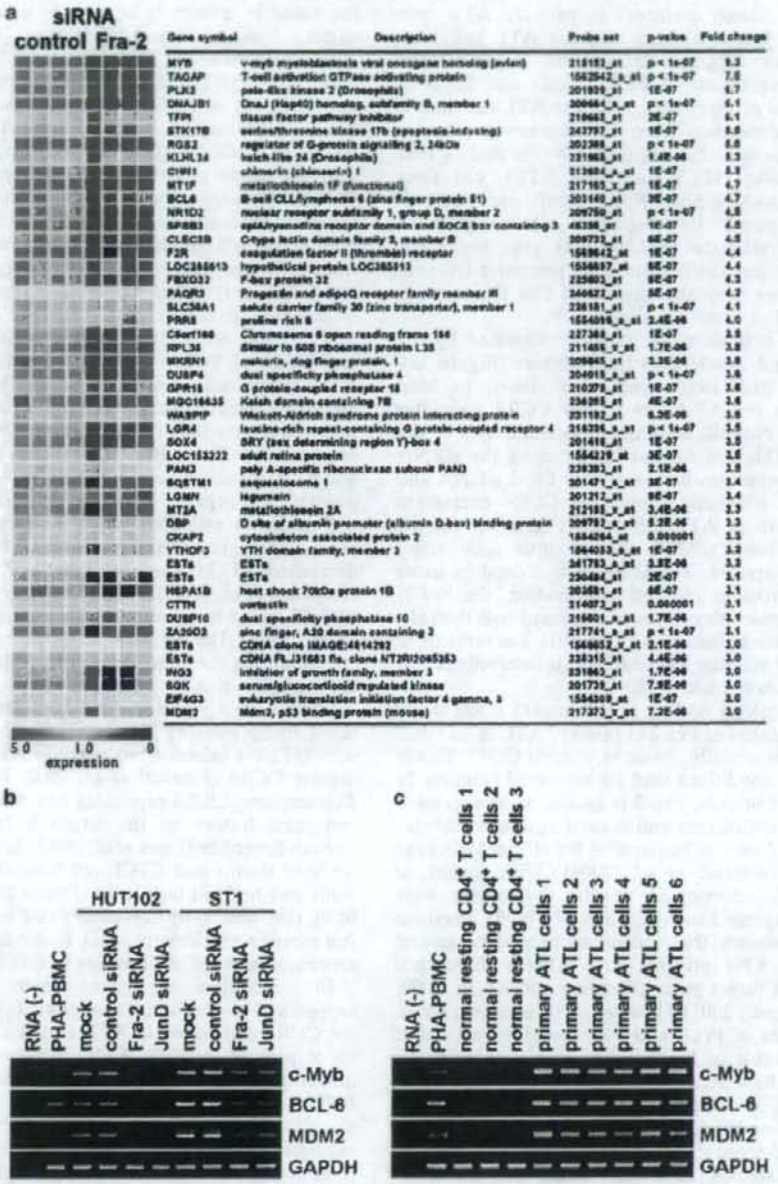

Gene symbol	Description	Probe set	p-value	Fold change
MYB	v-myb myeloblastosis viral oncogene homolog (avian)	2181152_at	p< 1e-07	9.3
TAGAP	T-cell activation GTPase activating protein	1562542_a_at	p< 1e-07	7.8
PLK2	polo-like kinase 2 (Drosophila)	201939_at	1E-07	6.7
DNAJB1	DnaJ (Hsp40) homolog, subfamily B, member 1	200664_s_at	p< 1e-07	6.1
TFPI	tissue factor pathway inhibitor	210665_at	2E-07	6.1
STK17B	serine/threonine kinase 17b (apoptosis-inducing)	243797_at	1E-07	5.8
RGS2	regulator of G-protein signalling 2, 24kDa	202388_at	p< 1e-07	5.6
KLHL24	kelch-like 24 (Drosophila)	231965_at	1.4E-06	5.3
CHN1	chimerin (chimaerin) 1	213624_x_at	1E-07	5.3
MT1F	metallothionein 1F (functional)	217165_x_at	1E-07	4.7
BCL6	B-cell CLL/lymphoma 6 (zinc finger protein 51)	203140_at	3E-07	4.7
NR1D2	nuclear receptor subfamily 1, group D, member 2	209750_at	p< 1e-07	4.6
SPSB3	spla/ryanodine receptor domain and SOCS box containing 3	46336_at	1E-07	4.6
CLEC3B	C-type lectin domain family 3, member B	209733_at	6E-07	4.5
F2R	coagulation factor II (thrombin) receptor	1569642_at	1E-07	4.4
LOC385513	hypothetical protein LOC385513	1556697_at	5E-07	4.4
FBXO32	F-box protein 32	225803_at	6E-07	4.3
PAQR3	Progestin and adipoQ receptor family member III	240672_at	5E-07	4.3
SLC38A1	solute carrier family 38 (zinc transporter), member 1	238181_at	p< 1e-07	4.1
PRR5	proline rich 5	1554098_a_at	2.4E-06	4.0
C6orf166	Chromosome 6 open reading frame 166	227368_at	1E-07	3.9
RPL35	similar to 60S ribosomal protein L35	211406_x_at	1.7E-06	3.8
MKRN1	makorin, ring finger protein, 1	1559845_at	3.3E-06	3.8
DUSP4	dual specificity phosphatase 4	204015_s_at	p< 1e-07	3.8
GPR15	G protein-coupled receptor 15	210279_at	1E-07	3.6
MGC16435	Kelch domain containing 7B	234265_at	4E-07	3.6
WASPIP	Wiskott-Aldrich syndrome protein interacting protein	231192_at	6.3E-06	3.6
LGR4	leucine-rich repeat-containing G protein-coupled receptor 4	218336_s_at	p< 1e-07	3.5
SOX4	SRY (sex determining region Y)-box 4	201416_at	1E-07	3.5
LOC153222	adult retina protein	1564239_at	3E-07	3.5
PAN3	poly A-specific ribonuclease subunit PAN3	239383_at	2.1E-06	3.5
SQSTM1	sequestosome 1	201471_s_at	3E-07	3.4
LGMN	legumain	201212_at	9E-07	3.4
MT2A	metallothionein 2A	212185_x_at	3.4E-06	3.3
DBP	D site of albumin promoter (albumin D-box) binding protein	209782_s_at	5.2E-06	3.3
CKAP2	cytoskeleton associated protein 2	1554264_at	0.000001	3.3
YTHDF3	YTH domain family, member 3	1554033_a_at	1E-07	3.3
ESTs	ESTs	241753_a_at	3.8E-06	3.3
ESTs	ESTs	230484_at	2E-07	3.1
HSPA1B	heat shock 70kDa protein 1B	203681_at	6E-07	3.1
CTTN	cortactin	214073_at	0.000001	3.1
DUSP10	dual specificity phosphatase 10	215601_s_at	1.7E-06	3.1
ZA20D3	zinc finger, A20 domain containing 3	217741_s_at	p< 1e-07	3.1
ESTs	CDNA clone IMAGE:4814292	1569652_x_at	2.1E-06	3.0
ESTs	CDNA FLJ31683 fis, clone NT2RI2005353	238315_at	4.4E-06	3.0
ING3	inhibitor of growth family, member 3	231863_at	1.7E-06	3.0
SGK	serum/glucocorticoid regulated kinase	201739_at	7.9E-06	3.0
EIF4G3	eukaryotic translation initiation factor 4 gamma, 3	1554309_at	1E-07	3.0
MDM2	Mdm2, p53 binding protein (mouse)	217373_x_at	7.2E-06	3.0

Figure 6 Identification of downstream target genes of Fra-2 in adult T-cell leukemia (ATL). (**a**) Microarray analysis. ST1 cells were transfected with control siRNA or Fra-2 siRNA. After 48 h, microarray analysis was performed using the Affymetrix GeneChip HG-U133 Plus 2.0 array. Four independent transfection samples were analysed for each group. Each column represents the expression level of a given gene in an individual sample. Red represents increased expression and blue represents decreased expression relative to the normalized expression of the gene across all samples. We computed the statistical significance level for each gene between the Fra-2-knockdown group and the control group with a mean fold change of > 3 by the *t*-test ($P<10^{-4}$). (**b**) Reverse transcription (RT)–PCR analysis. HUT102 and ST1 cells were transfected with control siRNA or siRNA for Fra-2 or JunD. After 48 h, the expression of c-Myb, BCL-6, MDM2 and GAPDH was determined by RT–PCR. The representative results from three separate experiments are shown. (**c**) RT–PCR analysis. Normal CD4+ T cells from healthy donors ($n=3$; purity, > 96%) and PBMC from ATL patients ($n=6$; leukemic cells, > 90%) were examined for the expression of c-Myb, BCL-6 and MDM2 by RT–PCR. The representative results from two separate experiments are shown.

various AP-1 family members in primary ATL cells (patient nos. 1 and 5) and in some ATL cell lines expressing Tax (Figures 2a and b). However, the constitutive expression of Fra-2, JunD and JunB in freshly isolated primary ATL cells and ATL cell lines is apparently independent from Tax expression (Figures 2a and b). This is further supported by the finding that CCR4-expressing HTLV-1-negative CTCL cell lines also constitutively express Fra-2, JunB and JunD at high levels (Figure 2). By using JPX-9, which is a subline of Jurkat carrying the HTLV-1 Tax gene under the control of the metallothionein gene promoter (Nagata *et al.*, 1989), we have also confirmed that Fra-2 is not inducible by Tax (data not shown).

The CCR4 promoter was potently activated by the Fra-2/JunB and Fra-2/JunD heterodimers (Figure 3a). Fra-2, JunB and JunD were also shown to bind specifically to the AP-1 site in the CCR4 promoter *in vitro* by the NoShift binding assays and *in vivo* by the ChIP assays (Figures 4a and b). By using the siRNA knockdown technique, however, only Fra-2 siRNA and JunD siRNA efficiently suppressed CCR4 expression and cell growth in ATL cell lines (Figure 5). On the other hand, JunB siRNA showed little such effect (Figure 5). Therefore, it is likely that, at least in terms of CCR4 expression and cell proliferation, the Fra-2/JunD heterodimer plays a more dominant role than the Fra-2/JunB heterodimer in ATL cells. It thus remains to be determined whether the Fra-2/JunB heterodimer has any specific functions in ATL.

The most striking finding in the present study is the aberrant expression of Fra-2 in primary ATL cells. Fra-2 expression is essentially absent in normal $CD4^+$ T cells under various conditions thus far examined (Figures 2a and c). Physiologically, Fra-2 is known to be expressed by various epithelial cells and in cartilaginous structures and has been shown to be required for efficient cartilage development (Karreth *et al.*, 2004). With regard to lymphoid cells, developing murine thymocytes were reported to express Fra-2 (Chen *et al.*, 1999). Previous studies have shown that individual homodimeric and heterodimeric AP-1 proteins have different functional properties and target genes (Shaulian and Karin, 2002; Eferl and Wagner, 2003). However, little is known about the target genes of Fra-2 and even less is known about the oncogenic role of Fra-2 in human malignancies. In this study, we have shown that CCR4 is the direct target gene of Fra-2 in association with JunD in ATL cells. Furthermore, we have shown that at least 49 genes are downregulated more than threefold in the ATL cell line ST-1 by Fra-2 siRNA (Figure 6). Among these genes, the proto-oncogenes c-Myb, BCL-6 and MDM2 (Oh and Reddy, 1999; Pasqualucci *et al.*, 2003; Vargas *et al.*, 2003) are further confirmed to be dependent on the Fra-2/JunD heterodimer and to be expressed at high levels in primary ATL cells (Figure 6). It remains to be seen whether the Fra-2/JunD heterodimer directly induces these proto-oncogenes or indirectly maintains their expression by promoting cell growth.

c-Myb is the genomic homologue of the avian myeloblastosis virus oncogene v-Myb. c-Myb is widely expressed in immature hematopoietic cells and also in various leukemias and carcinomas (Oh and Reddy, 1999; Shetzline *et al.*, 2004; Hess *et al.*, 2006). The target genes of c-Myb include the anti-apoptotic genes BCL-2 and BCL-X_L and also c-Myc (Ramsay *et al.*, 2003). Thus, c-Myb may promote the survival of ATL cells via BCL-2 and BCL-X_L (Galonek and Hardwick, 2006) and also cell cycle progression via c-Myc (Dang, 1999). BCL-6 was originally identified as the target gene of recurrent chromosomal translocations affecting 3q27 in non-Hodgkin's lymphoma. The expression of BCL-6 is frequently upregulated in diffuse large-cell lymphoma and follicular lymphoma through promoter substitution or somatic promoter point mutations (Ye *et al.*, 1993; Migliazza *et al.*, 1995; Chang *et al.*, 1996). Frequent expression of BCL-6 has also been reported in some T-cell lymphomas (Kerl *et al.*, 2001). The BCL-6 protein has been shown to exert cell-immortalizing and anti-senescence activities (Shvarts *et al.*, 2002; Pasqualucci *et al.*, 2003). Thus, BCL-6 may also inhibit apoptosis and promote cell cycle progression in ATL. The MDM2 protein is a negative regulator of p53 and suppresses p53-mediated cell cycle arrest and apoptosis (Vargas *et al.*, 2003). Elevated expression of MDM2 has been demonstrated in various types of human cancer (Rayburn *et al.*, 2005). Given that only a minor fraction of ATL cases have mutations affecting p53 (Cesarman *et al.*, 1992), the elevated expression of MDM2 may contribute to the functional downregulation of p53 in the majority of ATL cases.

CTCLs are a group of T-cell lymphomas derived from skin-homing memory T cells. CTCLs are not associated with HTLV-1 infection but resemble ATL and frequently express CCR4 (Ferenczi *et al.*, 2002; Kim *et al.*, 2005). Furthermore, CCR4 expression has been shown to be a consistent feature of the large-cell transformation of mycosis fungoides (Jones *et al.*, 2000). In the present study, we have shown that CTCL cell lines also express Fra-2, JunB and JunD at high levels (Figure 2b). Therefore, it is likely that aberrantly expressed Fra-2 in association with Jun proteins, particularly JunD, is also involved in CCR4-expression and cell proliferation in CTCLs.

In conclusion, we have shown that aberrantly expressed Fra-2 in association with JunD is responsible for CCR4 expression in ATL and is also likely to play an important role in ATL oncogenesis in part by inducing the expression of the proto-oncogenes c-Myb, BCL-6 and MDM2. Future studies are necessary to elucidate how the Fra-2/JunD heterodimer induces the expression of these proto-oncogenes and their individual roles in ATL oncogenesis. It also remains to be seen how ATL cells aberrantly express Fra-2 at high levels. Furthermore, the expression and function of Fra-2 in CTCLs remain to be determined.

Materials and methods

Cells

All the human T-cell lines used were described previously (Nagata *et al.*, 1989; Yamada *et al.*, 1996; Hata *et al.*, 1999;

Yoshie *et al.*, 2002). Peripheral blood mononuclear cells (PBMC) were isolated from heparinized blood samples obtained from healthy adult donors and acute ATL patients with a high leukemic cell count (>90%) by using Ficoll-Paque (Amersham Biosciences Corp, Piscataway, NJ, USA). Normal $CD4^+$ T cells (purity, >96%) were further prepared from PBMC by negative selection using an IMagnet system (BD Pharmingen, San Diego, CA, USA). Activated $CD4^+$ T cells were prepared by stimulating $CD4^+$ T cells with anti-CD3 (clone HIT3a; BD Pharmingen) and anti-CD28 (clone CD28.2; BD Pharmingen) for 24h. The preparation of naive $CD4^+CD45RA^+$ T cells and their polarization into Th1 and Th2 cells were performed as described previously (Imai *et al.*, 1999). Primary ATL cells and normal resting $CD4^+$ T cells were used without culture for the experiments. This study was approved by the local ethical committee and written informed consent was obtained from each patient.

Transfection and luciferase assay

The major transcriptional start site (+1) of the human CCR4 gene was determined by the method of rapid amplification of cDNA 5′-ends and was found to be located 1797 bases upstream from the translation start codon (data not shown). To generate a promoter–reporter construct, the 1-kb promoter region of the human CCR4 gene (−983 to +25) was amplified from the genomic DNA by PCR using primers based on a GenBank genomic DNA sequence (accession no. NC_000003) and inserted into the reporter plasmid pGL3-Basic (Promega, Madison, WI, USA). Deletions and site-directed mutations were also performed using PCR. pGL3-2xAP-1 was constructed by introducing a sequence containing two copies of the AP-1 consensus binding site (TGATGACTCAGCCG-GAATGATGACTCAGCC) in front of a minimal CCR4 promoter pGL3 (−96/+25; Figure 1b). The coding regions of human FosB and GATA-3 were amplified from a cDNA library generated from phytohemagglutinin (PHA)-stimulated PBMC by PCR and cloned into the expression vector pSG5 (Stratagene, La Jolla, CA, USA). The coding region of HTLV-1 HBZ was amplified from a cDNA library generated from the $HTLV\text{-}1^+$ T-cell line C8166 by PCR and cloned into the expression vector pEF4/myc-His A (Invitrogen, Carlsbad, CA, USA). The expression vectors for c-Fos, Fra-1, Fra-2, c-Jun, JunB, JunD and Tax were described previously (Iwai *et al.*, 2001). Cells (5×10^5) were transfected with 2 μg of reporter plasmid, 0.5 μg of expression plasmids for various transcription factors and 1 μg of pSV-β-galactosidase using DMRIE-C (Invitrogen). After 24–27h, luciferase assays were performed using a Luciferase Assay kit (Promega). Luciferase activity was normalized by β-galactosidase activity that served as an internal control for transfection efficiency.

RT–PCR

RT–PCR was carried out as described previously (Yoshie *et al.*, 2002). The primers used were as follows: +5′-AAGAA GAACAAGGCGGTGAAGATG-3′ and −5′-AGGCCCC TGCAGGTTTTGAAG-3′ for CCR4; +5′-TACTACCACTC ACCCGCAGACTC-3′ and −5′-CTTTTCCCTTCGGATTCT CCTTTT-3′ for c-Fos; +5′-TAGCAGCAGCTAAATGC AGGAAC-3′ and −5′-CCAGCTGAAGCCATCTTCCTT AG-3′ for FosB; +5′-CAGTGGATGGTACAGCCTCA TTT-3′ and −5′-GCCCAGATTTCTCATCTTCCAGT-3′ for Fra-1; +5′-CCAGCAGAAATTCCGGGTAGATA-3′ and −5′-TCTCCTCCTCTTCAGGAGACAGC-3′ for Fra-2; +5′-AAACAGAGCATGACCCTGAACCT-3′ and −5′-CTC CTGCTCATCTGTCACGTTCT-3′ for c-Jun; +5′-AAAAT GGAACAGCCCTTCTACCA-3′ and −5′-AGCCCTGACCA GAAAAGTAGCTG-3′ for JunB; +5′-AACACCCTTCT ACGGCGATGAG-3′ and −5′-GGGTAGAGGAACTGTG AGCTCGT-3′ for JunD; +5′-GAATTGGTGGACGGG CTATTATC-3′ and −5′-TAGCACTATGCTGTTTCGCCT TC-3′ for HBZ; +5′-CCGGCGCTGCTCTCATCCCGGT-3′ and −5′-GGCCGAACATAGTCCCCCAGAG-3′ for Tax; +5′-AAGGCATCCAGACCAGAAACCG-3′ and −5′-AGC ATCGAGCAGGGCTCTAACC-3′ for GATA-3; +5′-CAGT GACGAGGATGATGAGGACT-3′ and −5′-AACGTTTCG GACCGTATTTCTGT-3′ for c-Myb; +5′-ATTCCAGCTT CGGAACAAGAGAC-3′ and −5′-GTCCTTTTGATCAC TCCCACCTT-3′ for MDM2; +5′-CAAGAAGTTTCTAGG AAAGGCCGG-3′ and −5′-GATTGATCACACTAA GGTTGCATT-3′ for BCL-6 and +5′-GCCAAGGTCATCC ATGACAACTTTGG-3′ and −5′-GCCTGCTTCACCA CCTTCTTGATGTC-3′ for glyceraldehyde-3-phosphate dehydrogenase (GAPDH). The amplification conditions were denaturation at 94°C for 30s (5min for the first cycle), annealing at 60°C for 30s and extension at 72°C for 30s (5min for the last cycle) for 34 cycles for CCR4; 35 cycles for c-Fos, FosB, Fra-1, Fra-2, c-Jun, JunB, JunD, HBZ, Tax, c-Myb, BCL-6 and MDM2; 29 cycles for GATA-3 and 27 cycles for GAPDH. Amplification products were electrophoretically run on a 2% agarose gel and stained with ethidium bromide.

Quantitative real-time PCR was carried out using the TaqMan assay and a 7700 Sequence Detection System (Applied Biosystems, Foster City, CA, USA). The conditions for PCR were 50°C for 2min, 95°C for 10min and then 50 cycles of 95°C for 15s (denaturation) and 60°C for 1min (annealing extension). The primers and fluorogenic probes for CCR4 and 18S ribosomal RNA were obtained from a TaqMan kit (Applied Biosystems). Quantification of CCR4 expression was performed using the Sequence Detector System Software (Applied Biosystems).

NoShift transcription factor assay

Anti-c-Fos (sc-52), anti-FosB (sc-7203), anti-Fra-1 (sc-22794), anti-Fra-2 (sc-604), anti-c-Jun (sc-1694), anti-JunB (sc-73) and anti-JunD (sc-74) were purchased from Santa Cruz Biotechnology (Santa Cruz, CA, USA). Transcription factors bound to specific DNA sequences were identified using the NoShift Transcription Factor Assay Kit (EMD Biosciences, Madison, WI, USA). Nuclear extracts were prepared from human T-cell lines by using the NucBuster Protein Extraction Kit (EMD Biosciences). The oligonucleotides used were as follows (differences underlined): TGGGAAATGACTAAGAATCAT for the biotinylated probe and unlabeled competitor of the AP-1 site and TGGGAAATGTCAAAGAATCAT for the mutated AP-1 site.

ChIP assay

This assay was performed using a ChIP assay kit (Upstate Biotechnology, Lake Placid, NY, USA) following the manufacturer's instructions. In brief, cells (1×10^6) were cross-linked with 1% formaldehyde for 10min at room temperature. The cell pellets were lysed with sodium dodecyl sulfate (SDS) lysis buffer and sonicated to shear DNA to a size range between 200 and 1000 bp. After centrifugation, the supernatant was diluted 10-fold in ChIP dilution buffer and incubated overnight at 4°C with 4 μg of anti-Fra-2 (sc-604), anti-JunB (sc-73), anti-JunD (sc-74) or normal rabbit IgG (DAKO, Kyoto, Japan). Immunocomplexes were collected by adding protein A-agarose beads. The immune complexes were incubated at 65°C for 4h to reverse the protein/DNA cross-links. DNAs were then purified by phenol/chloroform extraction and used as templates for quantitative real-time PCR. The primers and

the fluorogenic probe for the AP-1 site of the CCR4 promoter were as follows: primers: +5′-GGTCTTGGGAAATGACT AAGAATCA-3′ and −5′-TCTCCCTCACCCAACTGTACT AAGT-3′; probe: 5′-TCTGCTTCCTACTTCTATCAAA AAACCCCACTTG-3′.

Immunological staining
Cells were spotted on a glass slide and fixed with 4% paraformaldehyde. Tissue sections were prepared from formalin-fixed and paraffin-embedded biopsy tissue samples and subjected to microwave irradiation for 5 min three times in Target Retrieval Solution (DAKO). Slides and tissue sections were incubated for 1 h at room temperature with anti-Fra-2 (sc-604), anti-JunB (sc-73), anti-JunD (sc-74) or mouse monoclonal anti-CCR4 (KM-2160; Kyowa Hakko, Tokyo, Japan). Normal rabbit IgG and control mouse IgG_1 (DAKO) were used as negative controls. After washing, the slides and tissue sections were incubated with biotin-labeled goat anti-rabbit IgG or biotin-labeled horse anti-mouse IgG followed by detection using the Vectastain ABC/HRP kit (Vector Laboratories, Burlingame, CA, USA). Finally, cells and sections were counterstained with Gill's hematoxylin (Polysciences, Warrington, PA, USA), dehydrated and mounted.

Transfection of siRNA
siRNAs for Fra-2 (SI00420455), JunB (SI03077445), JunD (SI00075985) and the negative control (1022064) were obtained from Qiagen (Hilden, Germany). Transfection experiments were performed using Amaxa Nucleofector (Amaxa, Cologne, Germany). Cells (1×10^6) were resuspended in 100 µl of Nucleofector solution (T solution for MOLT-4, HUT102 and ST1 and V solution for Jurkat) and transfected with 2.5 µg of siRNA using program O-17 for MOLT-4, HUT102 and ST1 and program S-18 for Jurkat. The transfection efficiency was ~95% as determined using fluorescent siRNA (Qiagen).

Cell proliferation assay
Cells were seeded in a 96-well plate at a density of 0.5×10^4 per well and cultured. The number of viable cells was determined every 24 h on a FACSCalibur system (Becton Dickinson, Mountain View, CA, USA) by gating out cells stained with propidium iodide. To prepare stable transfectants of Fra-2 and JunD, the coding regions of human Fra-2 and JunD were inserted into the pIRES2-EGFP vector (BD Biosciences, San Diego, CA, USA). Jurkat cells were transfected with the plasmids using DMRIE-C (Invitrogen). Stable transfectants expressing green fluorescence protein were sorted by flow cytometry using FACSVantage (Becton Dickinson).

Oligonucleotide microarray
Microarray analysis was performed as described previously (Igarashi *et al.*, 2007) using the Affymetrix GeneChip HG-U133 Plus 2.0 array (Affymetrix, Santa Clara, CA, USA). In brief, the ATL-derived cell line ST1 was transfected with control siRNA or Fra-2 siRNA. Four independent transfections were performed for each group. After 48 h, total RNA samples were prepared and confirmed to be of good quality with the Agilent 2100 Bioanalyzer (Agilent Technologies, Waldbronn, Germany). All microarray data have been submitted to the Gene Expression Omnibus (GEO; http://www.ncbi.nlm.nih.gov/geo; accession no. GSE6379). The analysis was performed using the BRB Array Tools software version 3.3.0 (http://linus.nci.nih.gov/BRB-ArrayTools.html) developed by Richard Simon and Amy Peng.

Acknowledgements

We thank Namie Sakiyama for her excellent technical assistance. We also thank Dr Rich Simon and Dr Amy Peng for providing the BRB ArrayTools software. This work was supported in part by a Grant-in-Aid from the Ministry of Education, Culture, Sports and Technology, Japan; by Solution-Oriented Research for Science and Technology (SORST) from Japan Science and Technology Corporation and by High-Tech Research Center Project for Private Universities: matching fund subsidy from the Ministry of Education, Culture, Sports, Science and Technology of Japan, 2002–2009.

References

Basbous J, Arpin C, Gaudray G, Piechaczyk M, Devaux C, Mesnard JM. (2003). The HBZ factor of human T-cell leukemia virus type I dimerizes with transcription factors JunB and c-Jun and modulates their transcriptional activity. *J Biol Chem* **278**: 43620–43627.

Cesarman E, Chadburn A, Inghirami G, Gaidano G, Knowles DM. (1992). Structural and functional analysis of oncogenes and tumor suppressor genes in adult T-cell leukemia/lymphoma shows frequent p53 mutations. *Blood* **80**: 3205–3216.

Chang CC, Ye BH, Chaganti RS, Dalla-Favera R. (1996). BCL-6, a POZ/zinc-finger protein, is a sequence-specific transcriptional repressor. *Proc Natl Acad Sci USA* **93**: 6947–6952.

Chen F, Chen D, Rothenberg EV. (1999). Specific regulation of fos family transcription factors in thymocytes at two developmental checkpoints. *Int Immunol* **11**: 677–688.

Dang CV. (1999). c-Myc target genes involved in cell growth, apoptosis, and metabolism. *Mol Cell Biol* **19**: 1–11.

Eferl R, Wagner EF. (2003). AP-1: a double-edged sword in tumorigenesis. *Nat Rev Cancer* **3**: 859–868.

Ferenczi K, Fuhlbrigge RC, Pinkus J, Pinkus GS, Kupper TS. (2002). Increased CCR4 expression in cutaneous T cell lymphoma. *J Invest Dermatol* **119**: 1405–1410.

Galonek HL, Hardwick JM. (2006). Upgrading the BCL-2 Network. *Nat Cell Biol* **8**: 1317–1319.

Grassmann R, Aboud M, Jeang KT. (2005). Molecular mechanisms of cellular transformation by HTLV-1 Tax. *Oncogene* **24**: 5976–5985.

Hata T, Fujimoto T, Tsushima H, Murata K, Tsukasaki K, Atogami S *et al.* (1999). Multi-clonal expansion of unique human T-lymphotropic virus type-I-infected T cells with high growth potential in response to interleukin-2 in prodromal phase of adult T cell leukemia. *Leukemia* **13**: 215–221.

Hess JL, Bittner CB, Zeisig DT, Bach C, Fuchs U, Borkhardt A *et al.* (2006). c-Myb is an essential downstream target for homeobox-mediated transformation of hematopoietic cells. *Blood* **108**: 297–304.

Hori S, Nomura T, Sakaguchi S. (2003). Control of regulatory T cell development by the transcription factor Foxp3. *Science* **299**: 1057–1061.

Iellem A, Mariani M, Lang R, Recalde H, Panina-Bordignon P, Sinigaglia F *et al.* (2001). Unique chemotactic response profile and specific expression of chemokine receptors CCR4 and CCR8 by CD4(+)CD25(+) regulatory T cells. *J Exp Med* **194**: 847–853.

Igarashi T, Izumi H, Uchiumi T, Nishio K, Arao T, Tanabe M *et al.* (2007). Clock and ATF4 transcription system regulates drug resistance in human cancer cell lines. *Oncogene* **26**: 4749–4760.

Imai T, Nagira M, Takagi S, Kakizaki M, Nishimura M, Wang J *et al.* (1999). Selective recruitment of CCR4-bearing Th2 cells toward antigen-presenting cells by the CC chemokines thymus and

activation-regulated chemokine and macrophage-derived chemokine. *Int Immunol* **11**: 81–88.

Ishida T, Utsunomiya A, Iida S, Inagaki H, Takatsuka Y, Kusumoto S *et al.* (2003). Clinical significance of CCR4 expression in adult T-cell leukemia/lymphoma: its close association with skin involvement and unfavorable outcome. *Clin Cancer Res* **9**: 3625–3634.

Iwai K, Mori N, Oie M, Yamamoto N, Fujii M. (2001). Human T-cell leukemia virus type 1 tax protein activates transcription through AP-1 site by inducing DNA binding activity in T cells. *Virology* **279**: 38–46.

Jeang KT, Chiu R, Santos E, Kim SJ. (1991). Induction of the HTLV-I LTR by Jun occurs through the Tax-responsive 21-bp elements. *Virology* **181**: 218–227.

Jones D, O C, Kraus MD, Perez-Atayde AR, Shahsafaei A, Wu L *et al.* (2000). Expression pattern of T-cell-associated chemokine receptors and their chemokines correlates with specific subtypes of T-cell non-Hodgkin lymphoma. *Blood* **96**: 685–690.

Karreth F, Hoebertz A, Scheuch H, Eferl R, Wagner EF. (2004). The AP1 transcription factor Fra2 is required for efficient cartilage development. *Development* **131**: 5717–5725.

Karube K, Ohshima K, Tsuchiya T, Yamaguchi T, Kawano R, Suzumiya J *et al.* (2004). Expression of FoxP3, a key molecule in CD4CD25 regulatory T cells, in adult T-cell leukaemia/lymphoma cells. *Br J Haematol* **126**: 81–84.

Kerl K, Vonlanthen R, Nagy M, Bolzonello NJ, Gindre P, Hurwitz N *et al.* (2001). Alterations on the 5′ noncoding region of the BCL-6 gene are not correlated with BCL-6 protein expression in T cell non-Hodgkin lymphomas. *Lab Invest* **81**: 1693–1702.

Kim EJ, Hess S, Richardson SK, Newton S, Showe LC, Benoit BM *et al.* (2005). Immunopathogenesis and therapy of cutaneous T cell lymphoma. *J Clin Invest* **115**: 798–812.

Matsubara Y, Hori T, Morita R, Sakaguchi S, Uchiyama T. (2005). Phenotypic and functional relationship between adult T-cell leukemia cells and regulatory T cells. *Leukemia* **19**: 482–483.

Matsuoka M. (2003). Human T-cell leukemia virus type I and adult T-cell leukemia. *Oncogene* **22**: 5131–5140.

Migliazza A, Martinotti S, Chen W, Fusco C, Ye BH, Knowles DM *et al.* (1995). Frequent somatic hypermutation of the 5′ noncoding region of the BCL6 gene in B-cell lymphoma. *Proc Natl Acad Sci USA* **92**: 12520–12524.

Mori N, Fujii M, Ikeda S, Yamada Y, Tomonaga M, Ballard DW *et al.* (1999). Constitutive activation of NF-kappaB in primary adult T-cell leukemia cells. *Blood* **93**: 2360–2368.

Mori N, Fujii M, Iwai K, Ikeda S, Yamasaki Y, Hata T *et al.* (2000). Constitutive activation of transcription factor AP-1 in primary adult T-cell leukemia cells. *Blood* **95**: 3915–3921.

Nagakubo D, Jin Z, Hieshima K, Nakayama T, Shirakawa AK, Tanaka Y *et al.* (2007). Expression of CCR9 in HTLV-1$^+$ T cells and ATL cells expressing Tax. *Int J Cancer* **120**: 1591–1597.

Nagata K, Ohtani K, Nakamura M, Sugamura K. (1989). Activation of endogenous c-fos proto-oncogene expression by human T-cell leukemia virus type I-encoded p40tax protein in the human T-cell line, Jurkat. *J Virol* **63**: 3220–3226.

Oh IH, Reddy EP. (1999). The myb gene family in cell growth, differentiation and apoptosis. *Oncogene* **18**: 3017–3033.

Pasqualucci L, Bereschenko O, Niu H, Klein U, Basso K, Guglielmino R *et al.* (2003). Molecular pathogenesis of non-Hodgkin's lymphoma: the role of Bcl-6. *Leuk Lymphoma* **44**(Suppl 3): S5–S12.

Ramsay RG, Barton AL, Gonda TJ. (2003). Targeting c-Myb expression in human disease. *Expert Opin Ther Targets* **7**: 235–248.

Rayburn E, Zhang R, He J, Wang H. (2005). MDM2 and human malignancies: expression, clinical pathology, prognostic markers, and implications for chemotherapy. *Curr Cancer Drug Targets* **5**: 27–41.

Rengarajan J, Szabo SJ, Glimcher LH. (2000). Transcriptional regulation of Th1/Th2 polarization. *Immunol Today* **21**: 479–483.

Satou Y, Yasunaga J, Yoshida M, Matsuoka M. (2006). HTLV-I basic leucine zipper factor gene mRNA supports proliferation of adult T cell leukemia cells. *Proc Natl Acad Sci USA* **103**: 720–725.

Shaulian E, Karin M. (2002). AP-1 as a regulator of cell life and death. *Nat Cell Biol* **4**: E131–E136.

Shetzline SE, Rallapalli R, Dowd KJ, Zou S, Nakata Y, Swider CR *et al.* (2004). Neuromedin U: a Myb-regulated autocrine growth factor for human myeloid leukemias. *Blood* **104**: 1833–1840.

Shvarts A, Brummelkamp TR, Scheeren F, Koh E, Daley GQ, Spits H *et al.* (2002). A senescence rescue screen identifies BCL6 as an inhibitor of anti-proliferative p19(ARF)-p53 signaling. *Genes Dev* **16**: 681–686.

Thebault S, Basbous J, Hivin P, Devaux C, Mesnard JM. (2004). HBZ interacts with JunD and stimulates its transcriptional activity. *FEBS Lett* **562**: 165–170.

Vargas DA, Takahashi S, Ronai Z. (2003). Mdm2: a regulator of cell growth and death. *Adv Cancer Res* **89**: 1–34.

Yamada Y, Ohmoto Y, Hata T, Yamamura M, Murata K, Tsukasaki K *et al.* (1996). Features of the cytokines secreted by adult T cell leukemia (ATL) cells. *Leuk Lymphoma* **21**: 443–447.

Yamamoto N, Hinuma Y. (1985). Viral aetiology of adult T-cell leukaemia. *J Gen Virol* **66**: 1641–1660.

Ye BH, Lista F, Lo Coco F, Knowles DM, Offit K, Chaganti RS *et al.* (1993). Alterations of a zinc finger-encoding gene, BCL-6, in diffuse large-cell lymphoma. *Science* **262**: 747–750.

Yoshida M. (2001). Multiple viral strategies of HTLV-1 for dysregulation of cell growth control. *Annu Rev Immunol* **19**: 475–496.

Yoshie O, Fujisawa R, Nakayama T, Harasawa H, Tago H, Izawa D *et al.* (2002). Frequent expression of CCR4 in adult T-cell leukemia and human T-cell leukemia virus type 1-transformed T cells. *Blood* **99**: 1505–1511.

Yoshie O, Imai T, Nomiyama H. (2001). Chemokines in immunity. *Adv Immunol* **78**: 57–110.

Antitumor activity of cetuximab against malignant glioma cells overexpressing EGFR deletion mutant variant III

Junya Fukai,[1,2] Kazuto Nishio,[3] Toru Itakura[2] and Fumiaki Koizumi[1,4]

[1]Shien-Laboratory, National Cancer Center Hospital, Tsukiji 5-1-1, Chuo-ku, Tokyo, 104-0045; [2]Department of Neurological Surgery, Wakayama Medical University, Kimiidera 811-1, Wakayama, 641-0012; [3]Department of Genome Biology, Kinki University School of Medicine, Ohno-higashi 377-2, Osaka-sayama, Osaka, 589-8511, Japan

(Received February 22, 2008/Revised June 17, 2008/Accepted June 19, 2008/Online publication October 3, 2008)

Anti-epidermal growth factor receptor (EGFR) monoclonal antibody, cetuximab, is a promising targeted drug for EGFR-expressing tumors. Glioblastomas frequently overexpress EGFR including not only the wild type but also a deletion mutant form called 'variant III (vIII)', which lacks exon 2–7, does not bind to ligands, and is constitutively activated. In this study, we investigated the antitumor activity of cetuximab against malignant glioma cells overexpressing EGFRvIII. For this purpose, we transfected human malignant glioma cell lines with the retroviral vector containing cDNA for EGFRvIII, and analyzed the mode of cetuximab-induced action on the EGFRvIII in the cells. Immunoprecipitation and immunofluorescence revealed binding of cetuximab to EGFRvIII. Notably, immunoblotting analyses showed that cetuximab treatment resulted in reduced expression levels of the EGFRvIII. However, cetuximab alone did not exhibit a growth-inhibitory effect against the EGFRvIII-expressing cells. On the other hand, an assay for antibody-dependent cell-mediated cytotoxicity (ADCC) demonstrated cetuximab-induced cytolysis in the presence of human peripheral blood mononuclear cells in a dose-dependent manner. These results suggest that deletion mutant EGFRvIII can be a target of cetuximab and that ADCC activity substantially contributes to the antitumor efficacy of cetuximab against the EGFRvIII-expressing glioma cells. Thus, cetuximab could be a promising therapy in malignant gliomas that express EGFRvIII. (*Cancer Sci* 2008; 99: 2062–2069)

Long-term survival of patients with malignant gliomas has not substantially improved despite aggressive multimodality treatments including cytoreductive surgery, radiotherapy, and cytotoxic chemotherapy. To efficiently suppress these tumors, additional therapeutic strategies are necessary. Understanding the molecular genetics, biology, and immunology of gliomas will enable the potential development of new adjuvant treatments for malignant glioma patients.

Malignant gliomas may arise via a heterogeneous process resulting from multiple genetic alterations.[1] One of the well-known molecular features of gliomas is amplification of the epidermal growth factor receptor (*EGFR*) gene, leading to overexpression of this receptor in approximately 40–60% of glioblastomas.[2,3] High levels of EGFR expression have been shown to be correlated with malignant progression in gliomas and associated with a poor prognosis and resistance to therapies.[4] Therefore, therapeutic strategies directed against the EGFR may have potential in these malignancies.

In the EGFR-amplified tumors, multiple types of EGFR mutations can be detected as a result of intragene deletions.[2] The most frequent mutation in malignant gliomas is EGFR variant III (EGFRvIII), characterized by a consistent and tumor-specific in-frame deletion of 801 base pairs from the coding sequence of the extracellular domain.[5,6] This mutated gene encodes a protein with a ligand-independent and constitutively active tyrosine kinase domain, which greatly enhances the tumorigenicity of the cells, mostly found *in vivo*, not *in vitro*.[7–9] The deletion mutant EGFRvIII, which is clonally expressed on the cell surface of ~40% of glioblastomas, has been clinically correlated with increased glioma cell growth, proliferation, invasion, and angiogenesis.[2,10,11] For the EGFR-targeted strategies in malignant glioma therapy, EGFRvIII expression should be considered because of its highly malignant nature.

Methods of targeting the EGFR that have been developed and trialed include monoclonal antibodies (mAbs), synthetic tyrosine kinase inhibitors, conjugates of toxins to anti-EGFR mAbs and ligands, and antisense gene therapy of EGFR.[12,13] Small molecule tyrosine kinase inhibitors and mAbs are the most fully developed of these approaches.[14,15]

Cetuximab (Erbitux, IMC-C225) is a recombinant, human-murine chimeric mAb specifically targeting the EGFR.[13] Cetuximab competes with endogenous ligands for binding to the extracelluar domain of EGFR and binding of cetuximab prevents stimulation of the receptor by ligands. Cetuximab-binding also results in internalization of the antibody-receptor complex which leads to down-regulation of EGFR expression on the cell surface.[13] Furthermore, this type of mAb including the human IgG1 Fc region may cause recruitment and activation of host immune-effector cells (T cells, natural-killer cells, and macrophages) or complements to induce antibody-dependent cell-mediated cytotoxicity (ADCC) or complement-dependent cytotoxicity (CDC).[16,17]

A variety of human epithelial cancers expressing EGFR have been successfully treated by cetuximab with promising results and it was recently approved for use in treating advanced-stage EGFR-expressing colorectal, head, and neck cancers.[13,18] However, little is known as to whether or not it is an effective therapy for the treatment of highly malignant tumors expressing deletion mutant EGFRvIII. Based on the encouraging results of cetuximab in the EGFR-expressing cancers and the importance of EGFRvIII expression in the biology of glioblastomas, we investigated whether cetuximab would be capable of effectively targeting the EGFRvIII expressed in malignant glioma cell lines.

Materials and Methods

Cell culture. Human glioblastoma cell lines were obtained as follows: U-251 MG, A-172, SF126, and YH-13, JCRB Cell Bank (Osaka, Japan); U-118 MG, U-87 MG, DBTRG-05 MG, LN-229,

*To whom correspondence should be addressed.
E-mail: fkoizumi@gan2.res.ncc.go.jp

doi: 10.1111/j.1349-7006.2008.00945.x

LN-18, and M059K, ATCC (Manassas, VA, USA). These cell lines were maintained in RPMI-1640 supplemented with 10% fetal bovine serum and cultured at 37°C in a humidified atmosphere containing 5% CO_2.

Expression vector construction and cell transfection. Construction of expression vector was generously contributed by Dr Hideyuki Yokote (Wakayama, Japan). Full-length cDNA of wild-type (wt) EGFR was amplified by reverse transcription–polymerase chain reaction (RT-PCR) from a human embryonal kidney cell line HEK293 using a High Fidelity RNA PCR Kit (TaKaRa, Shiga, Japan) and the following primer sets: forward, CGCTAGCGATGCGACCCTCCGGGAC; reverse, CCCCTGACTCCGTCCAGTATTGA. The PCR products were amplified using the following primer sets: forward, CGCTAGCGATGCGACCCTCCGGGAC; reverse, CGAAGCTTTGCTCCAATAAATTCACTGC. The amplified DNA included NheI- and HindIII-cut cohesive ends at the 5′- and 3′-ends, respectively. The product was subcloned into a pCR BluntII-TOPO vector (Invitrogen, Carlsbad, CA, USA) and the sequences were confirmed. Oligonucleotides encoding the myc-tag sequence (EQKLISEEDLN) were designed and synthesized as follows: forward, AGCTTGAACAGAAGCTGATCTCAGAGGAGGACCTGAATTGAC; reverse, TCGAGTCAATTCAGGTCCTCCTCTGAGATCAGCTTCTGTTCA. These oligos were annealed, and the ds-oligos were generated including HindIII- and XhoI-cut cohesive ends, at the 5′- and 3′-ends, respectively. Wt EGFR and myc-tag DNA fragments were cut out and transferred into a pQCXIX retroviral vector (BD Biosciences Clontech, San Diego, CA, USA) containing EGFP following internal ribosome entry site sequence. EGFRvIII was synthesized with the recombinant PCR method using the following primers: F1, CGCTAGCGATGCGACCCTCCGGGAC; R1, ATCTGTCACCACATAATTACCTTTCTTTTCCTCCAGAGCC; F2, GGCTCTGGAGGAAAAGAAAGGTAATTATGTGGTGACAGAT; R2, CGGTGGAGGTGAGGCAGATG. Two DNA fragments of wt EGFR were amplified using the F1/R1 and F2/R2 primer sets. The EGFR fragment deleting exon 2–7 was amplified using the two PCR products as templates and the F1/R2 primer set. After confirming the sequence, a wt EGFR fragment was substituted for the NheI- and EcoRI- cut recombinant PCR fragment. A pVSV-G vector (BD Biosciences Clontech) and the pQCXIX constructs were cotransfected into the GP2-293 cells (BD Biosciences Clontech) using a FuGENE6 transfection reagent (Roche Diagnostics, Basel, Switzerland). Briefly, 80% confluent cells cultured on a 10-cm dish were transfected with 2-mg pVSV-G plus 6-mg pQCXIX vectors. Forty-eight h after transfection, culture medium was collected and the viral particles were concentrated by centrifugation. The viral pellet was resuspended in fresh medium. The titer of the viral vector was calculated by counting the EGFP-positive cells which were infected by serial dilution of the virus-containing medium and the multiplicity of infection was determined.

Chemicals. Cetuximab was kindly provided by Brystol-Myers Squibb (Princeton, NJ, USA).

Antibodies. Abs were purchased as follows: antihuman EGFR mouse mAb cocktail, Biosource Corp. (Camarillo, CA, USA); antiphosphotyrosine mouse mAb, BD Biosciences; antiphospho-Akt, phospho-p44/42 mitogen activated protein kinase (MAPK), rabbit polyclonal, anti-β-actin rabbit monoclonal, and antimouse and rabbit IgG horseradish peroxidase–linked Abs, Cell Signaling Technology (Beverly, MA, USA).

Immunoblotting. Cells were seeded and grown to near confluency. Then, cells were washed with phosphate-buffered saline (PBS) and culture medium with or without cetuximab was added. At the time of harvest, cells were washed and lyzed with lysis buffer (50 mM Hepes buffer, 1% Triton X-100, 5 mM ethylenediaminetetraacetic acid [EDTA], 50 mM sodium chloride, 10 mM sodium pyrophosphate, 50 mM sodium fluoride, and 1 mM sodium orthovanadate) supplemented with protease inhibitors (Roche Diagnostics, Penzberg, Germany). Cell lysates were clarified by centrifugation, and equal concentrations of lysates were mixed with 4× sodium dodecyl sulfate (SDS)–gel sample buffer (0.25 mol/L Tris-HCl, pH 6.8, 2% SDS, and 25% glycerol), denatured with 2-mercaptoethanol. Equivalent amounts of protein were separated on SDS-polyacrylamide gels by electrophoresis, and transferred onto polyvinylidene difluoride (PVDF) membranes by wet electroblotting. The PVDF membranes were blocked with 3% bovine serum albumin in PBS with 0.1% Tween-20 and probed with primary Ab. The membranes were washed and incubated with secondary Ab. After the membranes were washed, immunoblotted proteins were detected using the ECL Western Blotting Detection System (GE Healthcare, Buckinghamshire, UK).

Immunoprecipitation. Cell lysates were extracted and treated with Ab overnight at 4°C. The lysates were mixed with protein A agarose and centrifuged. Immunoprecipitates were washed with lysis buffer and resuspended in 1.5× SDS-sample buffer and denatured with 2-mercaptoethanol. Samples were processed by immunoblotting.

Immunofluorescence. For immunofluorescence, cells were grown overnight, washed in PBS and fixed for 20 min in 4% paraformaldehyde at room temperature (RT). Cells were then washed twice in PBS and blocked for 1 h in 10% normal goat serum at RT. Cetuximab (10 mg/mL) was diluted in 1.5% normal goat serum and incubated overnight at 4°C. Cells were washed twice in PBS for 5 min and incubated with a secondary Ab for 45 min at RT. Secondary Abs included Alexa Fluor 546 Goat Anti-Mouse IgG (2 mg/mL; Molecular Probes, Invitrogen) and Texas Red antihuman IgG (1.5 mg/mL; Vector, Burlingame, CA, USA). Cells were washed twice for 5 min in PBS and then examined under a microscope (Keyence Biozero, Osaka, Japan).

Growth-inhibition assay (MTS assay). The growth-inhibitory effect of cetuximab was evaluated using the CellTiter96 Aqueous One Solution Cell Proliferation Assay (Promega Corporation, Madison, WI, USA). MTS (3-[4,5-dimethylthiazol-2-yl]-5-[3-carboxymethoxyphenyl]-2-[4-sulfophenyl]-2H-tetrazolium, inner salt) provides a measure of mitochondrial dehydrogenase activity within the cell and thereby offers an indication of cellular proliferation status.[19] Briefly, 3000 cells were seeded in 96-well plates. The plates were incubated overnight to permit adherence. Cells were then exposed to different concentrations of cetuximab ranging from 0 to 100 mg/mL for 48 h. MTS reagent was added and incubated for 1 h. The plates were read on a microplate spectrophotometer (optical density, 490 nm). The percentage cell growth was calculated by comparison of the absorbance value reading obtained from treated samples *versus* controls.

Antibody-dependent cell-mediated cytotoxicity (ADCC). Peripheral blood mononuclear cells (PBMCs) were separated from whole blood of healthy volunteers using LSM Lymphocyte Separation Medium (Cappel, Aurora, OH, USA). 1×10^5 cells were seeded into each well of a 12-well plate. After incubation for 24 h, human PBMCs alone (effector : target = 10:1), and/or cetuximab (10 mg/mL), control human IgG (10 mg/mL), or control medium were added to the wells. The cultures were then examined under a microscope (Keyence) 24-h post treatment.

Propidium iodide (PI) nucleic acid stain for cetuximab-mediated ADCC. This assay was performed for identifying dead cells in a population under the same experimental condition as described in the 'ADCC' section. A 4-μM solution of Cellstain PI (1 mg/mL; Dojindo, Kumamoto, Japan) was made at a dilution rate of 1:3000 and added per well. After incubation in the dark for 15 min, cells were viewed under a microscope (Keyence).

MTS assay for cetuximab-mediated ADCC. For analysis of the ADCC activity of cetuximab, we used the MTS assay.[20] Briefly, 3000 cells per well were exposed to various concentrations of cetuximab in the presence of PBMCs at an effector/target (E/T) ratio of 10 for 48 h. Natural killer (NK) activity was calculated from the absorbance value of the cells cultured without cetuximab

and PBMCs (A), the absorbance value of the cells cultured with PBMCs (B), the absorbance value of medium alone (C), and the absorbance value of PBMCs (D) as follows: $\{1 - [(B - C) - (D - C)]/[(A - C) - (D - C)]\} \times 100$. ADCC was calculated from the values of A, D, the NK activity (E), and the absorbance value of the cells treated with cetuximab and PBMCs (F): $\{1 - (F - D)/(A - D)\} \times 100 - E$.

Results

Initially, we determined the expression of endogenous EGFR protein in 10 human malignant glioma cell lines by immunoblotting (Fig. 1a). All of these malignant glioma cell lines displayed only low amounts of wt EGFR protein (170 kDa) but not EGFRvIII protein (145 kDa). These findings were consistent with the previous notion that because primary explants of human glioblastoma rapidly lose expression of amplified, rearranged receptors in culture, no existing glioblastoma cell lines exhibit such expression.[22] Therefore, we introduced the *EGFRvIII* gene into malignant glioma cell lines and engineered them to express this mutant receptor protein in three cell lines: U-251 MG, U-87 MG, and LN-229 (Fig. 1b). Malignant glioma cells that expressed the EGFRvIII protein were observed under fluorescence microscopy due to the coexpression of EGFP (Fig. 1c).

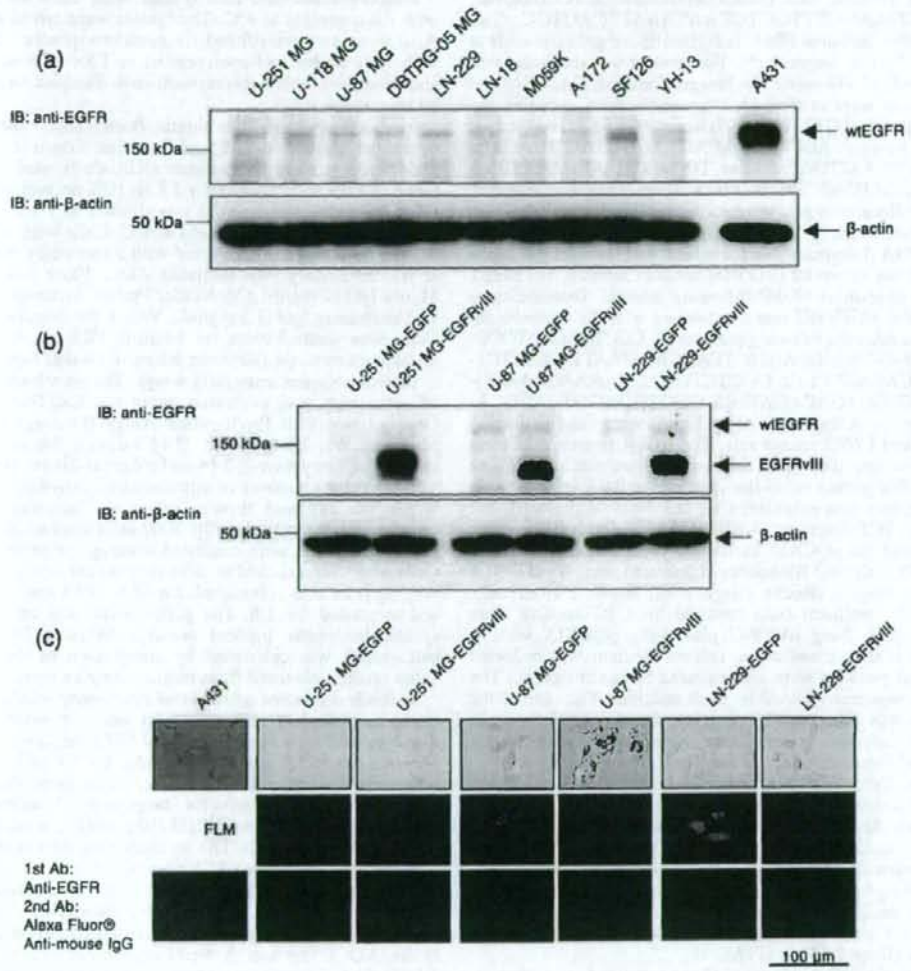

Fig. 1. (a) Expression of epidermal growth factor receptor (EGFR) in human malignant glioma cell lines. Ten malignant glioma cell lines were cultured and lyzed. Equal amounts of cell lysate were immunoblotted with anti-EGFR antibody (Ab) to show endogenous expression of EGFR. The human epidermoid carcinoma A431 cell lines served as a reference marker for high expression of wild-type (wt) EGFR.[21] Beta-actin showed protein loading. IB, immunoblotting. (b) Introduction of EGFRvIII into human malignant glioma cell lines. Three malignant glioma cell lines, into which the *EGFRvIII* gene was introduced, were cultured and lyzed. Equal amounts of cell lysates were immunoblotted with an anti-EGFR Ab to recognize exogenous expression of EGFRvIII. (c) Microscopic images and immunofluorescence of malignant glioma cells expressing EGFRvIII. EGFRvIII-expressing cells (*EGFRvIII*) were monitored by their coexpression of EGFP. Mock control (*EGFP*) expressed only EGFP. FM, fluorescent microscopy. EGFRvIII-expressing cells were stained with anti-EGFR Ab, then Alexa Fluor-conjugated antimouse IgG secondary Ab (lower panels). Staining of A431 or *EGFP* served as a reference of endogeneously expressed wt EGFR. Scale bar represents 100 μm.

doi: 10.1111/j.1349-7006.2008.00945.x

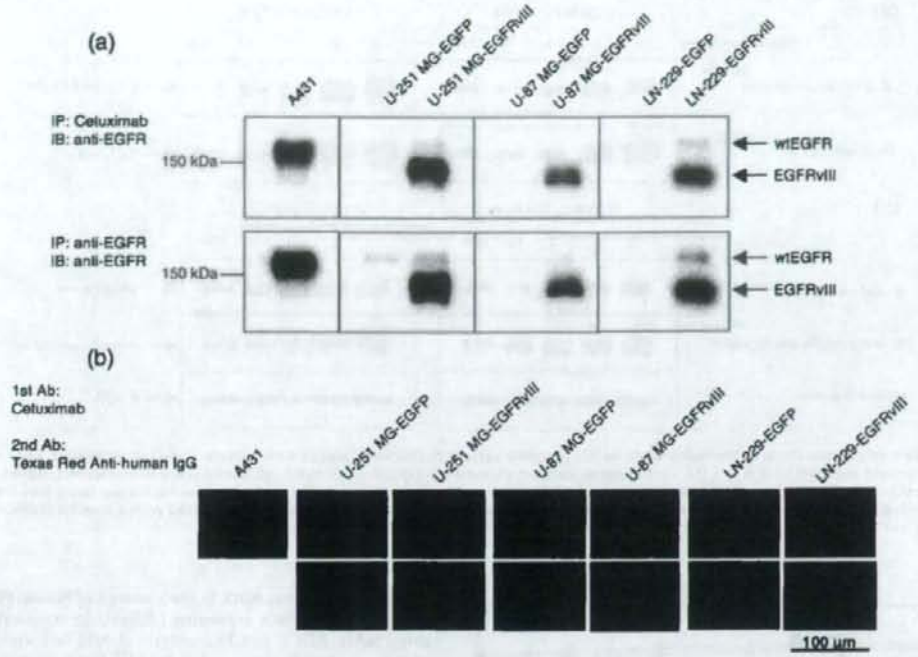

Fig. 2. (a) Immunoprecipitation showing cetuximab binding to epidermal growth factor receptor variant III (EGFRvIII). EGFRvIII-expressing cells were washed and lyzed. Equal amounts of cell lysates were immunoprecipitated with cetuximab or anti-EGFR antibody (Ab). The immunoprecipitates were probed by immunoblotting with anti-EGFR Ab. *A431* was used as a positive control for wild-type (wt) EGFR expression, and *EGFP* as a negative control for EGFRvIII. (b) Immunofluorescence showing cetuximab reactivity with malignant glioma cells expressing EGFRvIII. EGFRvIII-expressing cells were stained with cetuximab, then Texas Red–conjugated antihuman IgG secondary Ab. Staining of A431 or *EGFP* served as a reference for cetuximab reactivity with endogeneously expressed wt EGFR. Scale bar represents 100 μm.

Cetuximab has a binding ability to EGFRvIII. We investigated the binding capability of cetuximab to EGFRvIII by immunoprecipitation. Cell lysates were precipitated with cetuximab and then analyzed by immunoblotting with an anti-EGFR Ab. Cetuximab was found to precipitate the 140-kDa EGFRvIII protein from the EGFRvIII-expressing cells (Fig. 2a upper lane). There was no indication of an immunoreactive band migrating at the expected size of EGFRvIII in the mock control. The finding that the EGFRvIII protein was immunoprecipitated with cetuximab was confirmed by anti-EGFR Ab recognizing this mutant receptor (Fig. 2a lower lane).

Next, we performed immunofluorescence to investigate cetuximab reactivity with the EGFRvIII-overexpressing glioma cells. In this assay, cetuximab was used as a primary Ab, and Texas Red–conjugated antihuman IgG as a secondary Ab. In the mock control expressing low amounts of wt EGFR, we observed very low levels of staining, most of which were close to the detection limit of the analysis (Fig. 2b). In contrast, strong staining was evident in the EGFRvIII-overexpressing cells. Together these results demonstrate that cetuximab could recognize the deletion mutant EGFRvIII.

Cetuximab attenuates EGFRvIII expression and reduces phosphorylated EGFRvIII, but does not significantly inhibit Akt and MAPK signaling pathways. Based on the previous report that cetuximab-binding leads to down-regulation of EGFR expression, we investigated the effect of cetuximab on EGFRvIII expression by immunoblotting.[13] On treatment with cetuximab at various concentrations, the expression levels of EGFRvIII protein decreased dramatically in a dose-dependent manner (data not shown and Fig. 3a lower lane). In addition, we assessed the phosphorylation status of EGFRvIII by immunoprecipitation from the same lysates using a mAb recognizing EGFRvIII. The amount of immunoprecipitated EGFRvIII is shown in Fig. 3(a) (lower lane). A dose-dependent decrease in the expression of phosphorylated EGFRvIII was also observed, and the levels of tyrosine-phosphorylation corresponded to the expression of this receptor (Fig. 3a upper lane). Neither higher concentrations of cetuximab (= 100 μg/mL) nor prolonged exposure (72 h) augmented the effects on phosphorylated EGFRvIII expression (Fig. 3b and data not shown). Thus, cetuximab appeared to attenuate the EGFRvIII expression and reduce the phosphorylated EGFRvIII.

Next, we examined the phosphorylation status of Akt and MAPK pathways. On treatment with cetuximab, phosphorylated Akt and MAPK mildly decreased in the cells at higher concentrations (Fig. 3b). The decreased levels were not so significant as that of phosphorylated EGFRvIII. In summary, these results would suggest that when treated with cetuximab, EGFRvIII expression was markedly attenuated, while its downstream pathways by Akt and MAPK remained activated in the EGFRvIII-overexpressing glioma cells.

Cetuximab does not inhibit the growth of EGFRvIII-overexpressing glioma cells. We examined the effects of cetuximab on the growth of EGFRvIII-overexpressing glioma cells with an MTS assay. As can be observed in Fig. 4, cetuximab treatment did not produce a clear growth-inhibitory effect in the EGFRvIII-overexpressing cells even at the highest concentration tested. Also, treatment with cetuximab had a modest effect on the mock control. These data might support the findings determined by immunoblotting analyses.

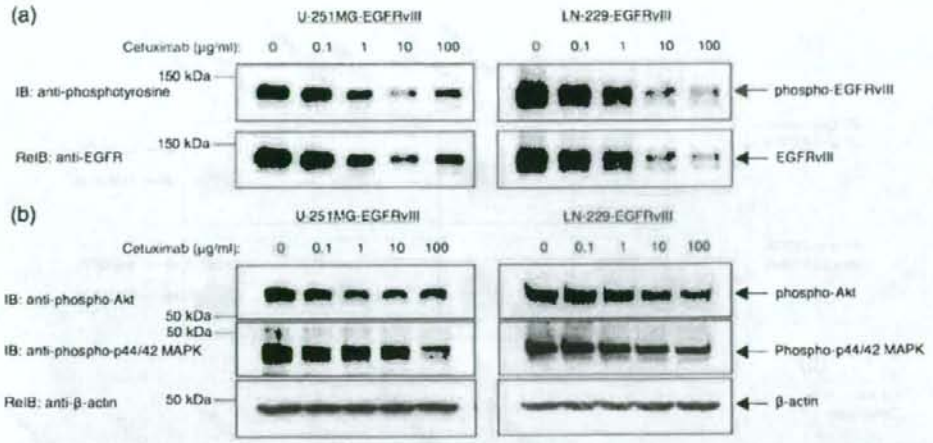

Fig. 3. Effect of cetuximab on epidermal growth factor receptor variant III (EGFRvIII) and its downstream signaling molecules. EGFRvIII-expressing glioma cells were exposed to 0, 0.1, 1, 10, or 100 μg/mL cetuximab for 24 h. (a) 250 μg of total cell lysates were immunoprecipitated with an anti-EGFR antibody (Ab). The immunoprecipitates were probed by immunoblotting with an antiphosphotyrosine Ab (upper lane) and the membranes were reblotted with an anti-EGFR antibody (lower lane). (b) Equal amounts of cell lysates were immunoblotted with a specific antihuman antibody as the first antibody, and then with a horseradish peroxidase–conjugated secondary antibody.

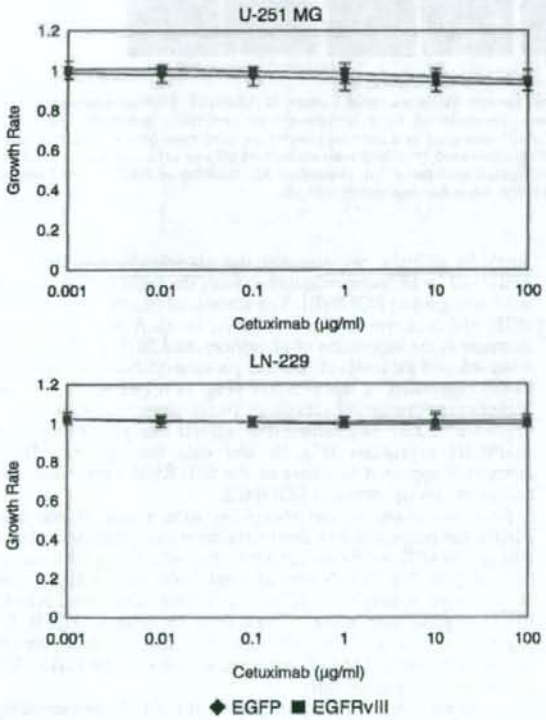

Fig. 4. MTS assays showing the growth-inhibitory effects of cetuximab on malignant glioma cells with and without epidermal growth factor receptor variant III (EGFRvIII) overexpression. 3000 glioma cells per well were placed onto a 96-well tissue culture plate and incubated overnight. Cetuximab was added at concentrations of 0–100 μg/mL and incubated for 48 h before an MTS assay was performed. This figure is representative of three independent experiments. Bars, SD.

Cetuximab induces ADCC in the presence of human PBMCs against malignant glioma cells expressing EGFRvIII. In molecular targeting using mAb, ADCC or CDC activity should be considered as one of the potent antitumor mechanisms.[16] First, we investigated the ADCC activity by morphological observation, PI stain, and an MTS assay. As our results in Fig. 5(a) show, cetuximab in the presence of PBMCs induced extensive lysis of the cells in culture. In contrast, treatment with cetuximab alone, human PBMCs alone, or PBMCs plus human IgG control (data not shown), did not apparently induce lysis of the cells. Correspondingly, PI nucleic acid stain revealed remarkable cell death in the cell population treated with cetuximab and PBMCs (Fig. 5b). To further evaluate cetuximab-induced ADCC against EGFRvIII expressed in the cells, we performed the MTS assay in the presence of human PBMCs at an E/T ratio of 10. In the mock control with low expression levels of wt EGFR, mild ADCC activity was detected (Fig. 5c). On the other hand, cetuximab treatment significantly inhibited the proliferation of the EGFRvIII-overexpressing glioma cells in a dose-dependent manner. There was no significant percentage ADCC at the zero μg/mL of cetuximab in the EGFRvIII-expressing cells as well as in mock controls (EGFP), suggesting that both cells could not be susceptible to PBMCs alone. Next, we examined CDC activity against these cells using the MTS assay in the presence of 25% human serum containing human complement. No CDC-mediated cytolytic effect was observed even at the highest concentration of cetuximab tested (data not shown). These results suggest that this mAb also recognizes the EGFRvIII expressed on the cell surfaces and exerts potent ADCC activity against the glioma cells overexpressing this mutant receptor.

Discussion

Overexpression of EGFR can be a promising characteristic as a molecular target for malignant glioma therapy.[12] Malignant gliomas that are wt EGFR–positive may simultaneously overexpress EGFRvIII, which is reported to be associated with aggressive phenotypes and resistance to chemo- and radiotherapy.[2,10,11] Although anti-EGFR mAb cetuximab may play an important role and be hopefully evaluated in preclinical studies, limited

doi: 10.1111/j.1349-7006.2008.00945.x

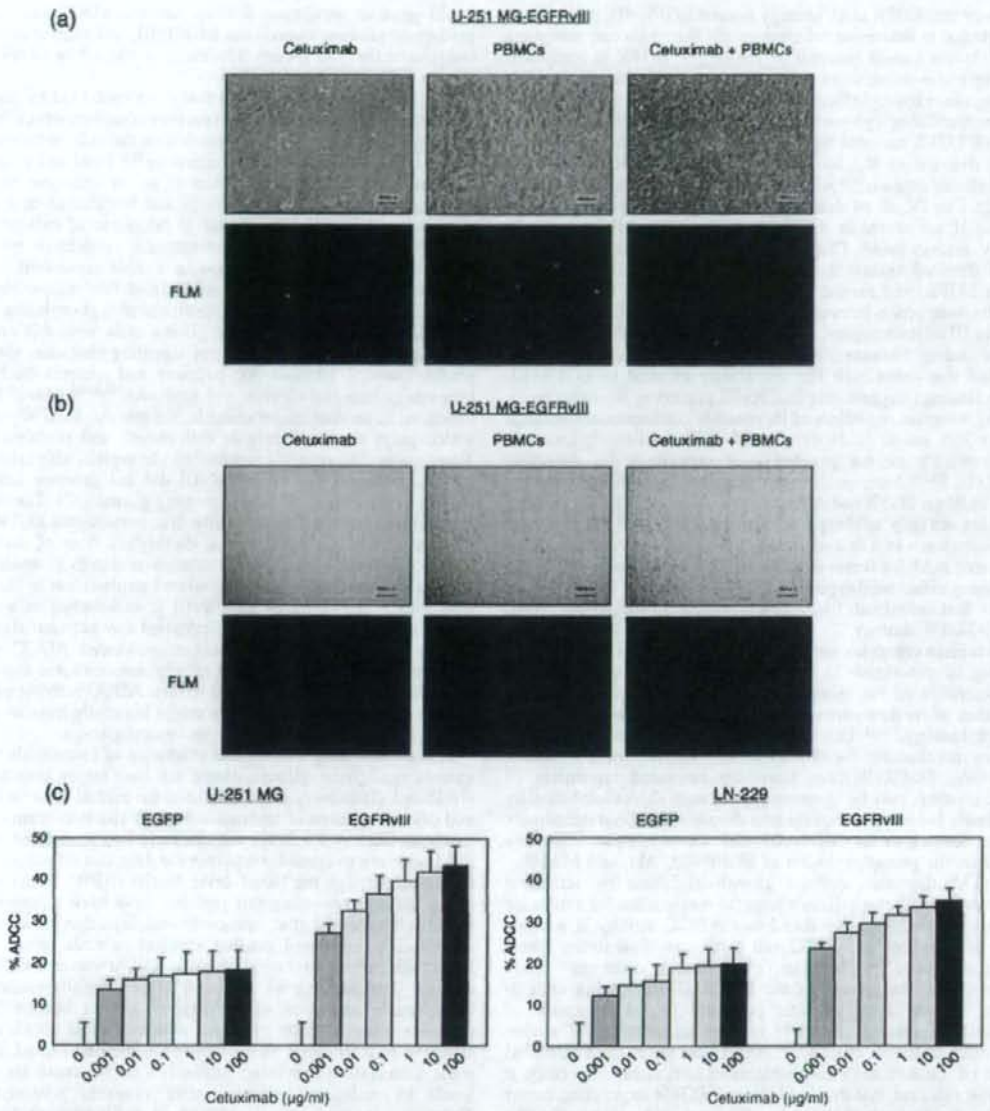

Fig. 5. (a) Microscopic findings showing cetuximab-mediated antibody-dependent cell-mediated cytotoxicity (ADCC) of glioma cells expressing epidermal growth factor receptor variant III (EGFRvIII). Monolayers of the glioma cells were treated with cetuximab (10 μg/mL) and human peripheral blood mononuclear cells (PBMCs) at an effector target ratio of 10:1 at 37°C for 24 h. Controls included treatment with cetuximab alone (left panels), PBMCs alone (middle panels), or PBMCs plus human IgG (data not shown). Note the extensive lysis of the cells in the presence of both cetuximab and PBMC (right panels) but not in any of the control cultures. (b) Propidium iodide (PI) stain showing cetuximab-mediated ADCC of the EGFRvIII-expressing glioma cells. Under the same condition as (a), PI solution was added and incubated for 15 min. Note the remarkable increase of the dead cells in the presence of both cetuximab and PBMC (right panels). (c) MTS assays showing the ADCC activity of cetuximab against malignant glioma cells with and without EGFRvIII expression. Under the same condition as in Fig. 4, human PBMCs were added at an effector target ratio of 10:1 and incubated for 48 h before an MTS assay was performed. This figure is representative of three independent experiments. Bars, SD.

data have been reported regarding the potential of cetuximab to target the EGFRvIII in malignant glioma cells.[3] The present data provide evidence that cetuximab has a capability to recognize EGFRvIII as well as wt EGFR. Although cetuximab produces modest activities to block the EGFRvIII signaling or inhibit the growth of glioma cells with this receptor directly, this mAb has great potential to induce ADCC activity against the EGFRvIII-expressing glioma cells. These results suggest that cetuximab therapy might be effective against malignant gliomas expressing EGFRvIII.

In any anti-EGFR mAb strategy against EGFRvIII, it is of great importance to determine whether or not the mAb can recognize this deletion mutant receptor as the target. EGFR is composed of three major domains: extracellular domains including a ligand-binding site, a hydrophobic transmembrane segment, and a tyrosine-kinase containing cytoplasmic region.[13] EGFRvIII is a mutant form of EGFR encoded by a mutated gene characterized by in-frame deletion of 801 bp coding 6–273 amino acids from the extracellular domain.[11] As the extracellular part is composed of domain I to IV, all of domain I and the amino-terminal 2/3 of domain II are absent in this mutant receptor, while domain III and IV remain intact. Cetuximab has been produced as one of mAbs directed against the extracellular ligand-binding domain of the EGFR, and recent structural studies have demonstrated that the interaction between cetuximab and the EGFR is with domain III of the receptor, not with other domains.[18] Our experiments using immunoprecipitation and immunofluorescence revealed that cetuximab has the ability to bind to EGFRvIII. These findings suggest that EGFRvIII preserves the cetuximab-binding structure regardless of its possible conformational change due to 268 amino acids deletion.[18,23] There have been some recent reports on the possibility of cetuximab for detecting EGFRvIII.[24,25] Aerts *et al.* developed cetuximab-based imaging probe to target EGFR and demonstrated its potential as an imaging agent for not only wild type but also EGFRvIII.[24] Yang's group used cetuximab as a delivery tool of radio-isotope and evaluated boronated mAb for boron neutron capture therapy of a rat glioma expressing either wild-type EGFR or EGFRvIII.[25] This evidence reveals that cetuximab has a potential role in the advancement of anti-EGFR strategy.

Cetuximab competes with ligands for binding to the EGFR.[13] Binding of cetuximab to the EGFR prevents phosphorylation and activation of the receptor tyrosine kinase, resulting in the inhibition of its downstream signal transduction which controls cellular biology.[13,14] This mode of action is considered as the primary mechanism for the antitumor activity of cetuximab. Therefore, EGFRvIII, constitutively activated regardless of ligand-binding, may be insusceptible to such direct inhibition by cetuximab. Indeed, our experiments demonstrated that cetuximab, despite binding to the EGFRvIII, did not have clear inhibitory effects on the phosphorylation of EGFRvIII, Akt, and MAPK.

In mAb therapies, indirect growth-inhibition by activating host immune effector cells is a hopeful mechanism for antitumor activity.[16] Previously, we found that ADCC activity is a major mode of action of anti-HER2/neu mAb trastuzumab for breast cancer cell lines.[20] Therefore, even though cetuximab alone cannot inhibit the growth of the EGFRvIII-expressing cells in culture, it may have cytolitic potential in the treatment of EGFRvIII-expressing tumors *in vivo* by immunological mechanisms such as ADCC or CDC.[26] ADCC has rarely been discussed as one of the antitumor mechanisms of cetuximab. Recently, it has been reported that this mAb causes EGFR-expressing tumor cells to die through this mode of action and elicits effective ADCC activity against lung, head, and neck cancer.[17,27,28] In the literature, the authors describe the potential of cetuximab to exhibit ADCC activity mediated by targeting EGFR expressed in tumor cells, but do not discuss in detail whether cetuximab-mediated ADCC can be evoked against mutant EGFR, especially a deletion mutant form of extracellular domain that is vital for cetuximab binding, which is often discussed in malignant glioma. Our *in vitro* study showed that in the presence of human PBMCs, cetuximab induced strong ADCC, presumably due to additional activation of the immune effector functions by this antibody. A new insight drawn from our study is that even though the target is EGFRvIII, which has a partial deletion of EGF-binding site, once cetuximab binds to the mutant receptor, ADCC could be substantially produced against malignant glioma cells. These findings suggest that *in vivo* treatment of cetuximab could generate antitumor activity through ADCC even against malignant gliomas expressing EGFRvIII, although it should be considered that the growth advantage conferred by EGFRvIII is mostly found *in vivo*, not *in vitro*.

Previous studies have shown that cetuximab binding results in internalization of the antibody-receptor complex, which leads to down-regulation of EGFR expression on the cell surface and the blockading of its downstream signaling.[13] Patel and colleagues examined the ability of cetuximab as an effective drug for EGFRvIII-expressing tumor cells and concluded that down-regulation of EGFRvIII resulted in inhibition of cell proliferation.[29] In our experimental conditions, cetuximab treatment attenuated EGFRvIII expression in a dose-dependent manner. However, despite the decreased levels of this mutant receptor, cetuximab did not apparently inhibit the phosphorylation of Akt and MAPK and the growth of glioma cells with this receptor. Akt functions in one of the major signaling cascades, the phosphatidylinositol-3-kinase-Akt pathway, and controls the balance between glioma cell survival and apoptosis.[13,30,31] p44/42 MAPK functions in another major cascade, the ras–raf–MAPK pathway, which plays a critical role in cell growth and proliferation.[13] There are several possible mechanisms to explain why cetuximab-mediated attenuation of EGFRvIII did not produce antitumor activity in the EGFRvIII-overexpressing glioma cells. The simplest explanation rests in the possibility that, because the EGFRvIII is not completely depleted even at the highest dose of cetuximab tested, EGFRvIII signaling still exists to maintain its downstream activation. Another potentially related explanation is that once constitutive activation of EGFRvIII is established in a cell, it may be difficult to disturb the constant downstream signaling. In any case, we expected cetuximab-induced ADCC against EGFRvIII-expressing cells and clearly demonstrated that cetuximab binding to EGFRvIII could exhibit ADCC activity, inducing glioma cell death. This evidence might hopefully have an impact in anti-EGFR mAb therapy for malignant glioma.

When discussing the clinical relevance of cetuximab therapy against malignant glioma, there are two major points to be elucidated: (i) delivery of cetuximab to the central nervous system; and (ii) recruitment of immune-effector cells into brain tumors. In chemotherapy for brain tumors including malignant glioma, it is necessary to consider whether the drug can effectively reach the tumor through the blood–brain barrier (BBB). Some encouraging findings regarding this problem have been reported. Eller *et al.* demonstrated that intraperitoneal injection of cetuximab significantly increased median survival in nude mice bearing intracranial xenografts of glioblastoma.[3] Arwert and colleagues showed that intravenous injection of cetuximab resulted in a considerable reduction of intracranial glioma burden.[32] This evidence suggests that systemic administration could achieve effective concentration in the brain. On the other hand, there is some information that intact antibodies do not reach significant levels in malignant gliomas after systemic administration. Therefore, in the clinical practice of mAb therapy for brain tumors, several methods to deliver the agent to tumors have been tried out, such as convection-enhanced delivery with stereotactic infusion-catheter placement and osmotic BBB disruption with selective intra-arterial mannitol infusion, producing promising results. Recently, non-invasive localized delivery of mAb to the mouse brain was reported by magnetic resonance imaging–guided focused ultrasound-BBB disruption.[33] These modalities would enable effective delivery of cetuximab to malignant gliomas in the brain. Next, recruitment of immune-effector cells into the brain tumor is also vital for cetuximab to induce ADCC reaction against malignant glioma. In previous literature on mAb treatment for brain tumors, peritumoral infiltrates of macrophages were shown in mice treated with the mAb which was found to induce ADCC *in vitro*, whereas a paucity of T cells and natural killer cells was also described.[34] Although it should be elucidated

doi: 10.1111/j.1349-7006.2008.00945.x

whether macrophages or microglia would be able to mediate the ADCC in the brain, the promising result in the paper suggested that the mAb-mediated ADCC reaction could be evoked in *in vivo* models, which might be encouraging for cetuximab to produce an effective ADCC activity *in vivo*. In conclusion, the above information provides us with some hope that cetuximab may be used to treat patients with malignant glioma. As the next step, further investigation is needed in a clinical setting.

In summary, we have reported that cetuximab can target EGFRvIII and although this mAb appears to be less effective in direct inhibition of EGFRvIII activity, intervention of effector cells such as human PBMCs can produce antitumor efficacy of cetuximab even against EGFRvIII-expressing glioma cells. In view of the concept that cetuximab has been previously shown to develop chemosensitizing and radiosensitizing effects, the use of this mAb may have great therapeutic potential against malignant gliomas.[3,4] Moreover, conjugation of cytotoxic agents such as drugs or radioisotopes might produce enhanced antitumor activity.[12] Thus, we emphasize that targeted therapy using the anti-EGFR mAb cetuximab could play a significant role in the development of multidisciplinary treatment strategies for these tumors.

Acknowledgments

This work was partially supported by funds from the Third Term Comprehensive 10-Year Strategy for Cancer Control (N.K. and K.F.) and Health and Labor Sciences Grants, Research on Advanced Medical Technology, H17-Pharmaco-006 (N.K. and K.F.).

We thank Brystol-Myers Squibb (cetuximab) for providing the anti-EGFR agents for experimental studies.

References

1 von Deimling A, Louis DN, Wiestler OD. Molecular pathways in the formation of gliomas. *Glia* 1995; **15**: 328–38.
2 Frederick L, Wang XY, Eley G, James CD. Diversity and frequency of epidermal growth factor receptor mutations in human glioblastomas. *Cancer Res* 2000; **60**: 1383–7.
3 Eller JL, Longo SL, Kyle MM, Bassano D, Hicklin DJ, Canute GW. Anti-epidermal growth factor receptor monoclonal antibody cetuximab augments radiation effects in glioblastoma multiforme in vitro and in vivo. *Neurosurgery* 2005; **56**: 155–62.
4 Eller JL, Longo SL, Hicklin DJ, Canute GW. Activity of anti-epidermal growth factor receptor monoclonal antibody C225 against glioblastoma multiforme. *Neurosurgery* 2002; **51**: 1005–14.
5 Sugawa N, Ekstrand AJ, James CD, Collins VP. Identical splicing of aberrant epidermal growth factor receptor transcripts from amplified rearranged genes in human glioblastomas. *Proc Natl Acad Sci USA* 1990; **87**: 8602–6.
6 Wong AJ, Ruppert JM, Bigner SH *et al.* Structural alterations of the epidermal growth factor receptor gene in human gliomas. *Proc Natl Acad Sci USA* 1992; **89**: 2965–9.
7 Nishikawa R, Ji XD, Harmon RC *et al.* A mutant epidermal growth factor receptor common in human glioma confers enhanced tumorigenicity. *Proc Natl Acad Sci USA* 1994; **91**: 7727–31.
8 Batra SK, Castelino-Prabhu S, Wikstrand CJ *et al.* Epidermal growth factor ligand-independent, unregulated, cell-transforming potential of a naturally occurring human mutant EGFRvIII gene. *Cell Growth Differ* 1995; **6**: 1251–9.
9 Huang HS, Nagane M, Klingbeil CK *et al.* The enhanced tumorigenic activity of a mutant epidermal growth factor receptor common in human cancers is mediated by threshold levels of constitutive tyrosine phosphorylation and unattenuated signaling. *J Biol Chem* 1997; **272**: 2927–35.
10 Nagane M, Coufal F, Lin H, Bogler O, Cavenee WK, Huang HJ. A common mutant epidermal growth factor receptor confers enhanced tumorigenicity on human glioblastoma cells by increasing proliferation and reducing apoptosis. *Cancer Res* 1996; **56**: 5079–86.
11 Learn CA, Hartzell TL, Wikstrand CJ *et al.* Resistance to tyrosine kinase inhibition by mutant epidermal growth factor receptor variant III contributes to the neoplastic phenotype of glioblastoma multiforme. *Clin Cancer Res* 2004; **10**: 3216–24.
12 Halatsch ME, Schmidt U, Behnke-Mursch J, Unterberg A, Wirtz CR. Epidermal growth factor receptor inhibition for the treatment of glioblastoma multiforme and other malignant brain tumours. *Cancer Treat Rev* 2006; **32**: 74–89.
13 Harding J, Burtness B. Cetuximab. An epidermal growth factor receptor chimeric human-murine monoclonal antibody. *Drugs Today* 2005; **41**: 107–27.
14 Herbst RS, Shin DM. Monoclonal antibodies to a target epidermal growth factor receptor-positive tumors. *Cancer* 2002; **94**: 1593–611.
15 Wakeling AE. Epidermal growth factor receptor tyrosine kinase inhibitors. *Curr Opin Pharmacol* 2002; **2**: 382–7.
16 Harris M. Monoclonal antibodies as therapeutic agents for cancer. *Lancet Oncol* 2004; **5**: 292–302.
17 Kimura H, Sakai K, Arao T, Shimoyama T, Tamura T, Nishio K. Antibody-dependent cellular cytotoxicity of cetuximab against tumor cells with wild-type or mutant epidermal growth factor receptor. *Cancer Sci* 2007; **98**: 1275–80.
18 Li S, Schmitz KR, Jeffrey PD, Wiltzius JJW, Kussie P, Ferguson KM. Structural basis for inhibition of the epidermal growth factor receptor by cetuximab. *Cancer Cell* 2005; **7**: 301–11.
19 Huang S, Armstrong EA, Benavente S, Chinnaiyan P, Harari PM. Dual-agent molecular targeting of the epidermal growth factor receptor (EGFR): combining anti-EGFR antibody with tyrosine kinase inhibitor. *Cancer Res* 2004; **64**: 5355–62.
20 Naruse I, Fukumoto H, Saijo N, Nishio K. Enhanced anti-tumor effect of trastuzumab in combination with cisplatin. *Jpn J Cancer Res* 2002; **93**: 574–81.
21 Perera RM, Narita Y, Furnari FB *et al.* Treatment of human tumor xenografts with monoclonal antibody 806 in combination with a prototypical epidermal growth factor receptor-specific antibody generates enhanced antitumor activity. *Clin Cancer Res* 2005; **11**: 6390–9.
22 Mishima K, Johns TG, Luwor RB *et al.* Growth suppression of intracranial xenografted glioblastomas overexpressing mutant epidermal growth factor receptors by systemic administration of monoclonal antibody (mAb) 806, a novel monoclonal antibody directed to the receptor. *Cancer Res* 2001; **61**: 5349–54.
23 Garrett TP, McKern NM, Lou M *et al.* Crystal structure of a truncated epidermal growth factor receptor extracellular domain bound to transforming growth factor alpha. *Cell* 2002; **110**: 763–73.
24 Aerts HJ, Dubois L, Hackeng TM *et al.* Development and evaluation of a cetuximab-based imaging probe to target EGFR and EGFRvIII. *Radiother Oncol* 2007; **83**: 326–32.
25 Yang W, Wu G, Barth RF *et al.* Molecular targeting and treatment of composite EGFR and EGFRvIII positive gliomas using boronated monoclonal antibodies. *Clin Cancer Res* 2008; **14**: 883–91.
26 Modjtahedi H, Moscatello DK, Box G *et al.* Targeting of cells expressing wild-type EGFR and type-III mutant EGFR (EGFRvIII) by anti-EGFR MAb ICR62: a two-pronged attack for tumour therapy. *Int J Cancer* 2003; **105**: 273–80.
27 Kurai J, Chikumi H, Hashimoto K *et al.* Antibody-dependent cellular cytotoxicity mediated by cetuximab against lung cancer cell lines. *Clin Cancer Res* 2007; **13**: 1552–61.
28 Astsaturov I, Cohen RB, Harari P *et al.* EGFR-targeting monoclonal antibodies in head and neck cancer. *Curr Cancer Drug Targets* 2007; **7**: 650–65.
29 Patel D, Lahiji A, Patel S *et al.* Monoclonal antibody cetuximab binds to and down-regulates constitutively activated epidermal growth factor receptor vIII on the cell surface. *Anticancer Res* 2007; **27**: 3355–66.
30 Matar P, Rojo F, Cassia R *et al.* Combined epidermal growth factor receptor targeting with the tyrosine kinase inhibitor gefitinib (ZD1839) and the monoclonal antibody cetuximab (IMC-C225): superiority over single-agent receptor targeting. *Clin Cancer Res* 2004; **10**: 6487–501.
31 Mellinghoff IK, Wang MY, Vivanco I *et al.* Molecular determinants of the response of glioblastomas to EGFR kinase inhibitors. *N Engl J Med* 2005; **353**: 2012–24.
32 Arwert E, Hingtgen S, Figueiredo J-L *et al.* Visualizing the dynamics of EGFR activity and antiglioma therapies *in vivo*. *Cancer Res* 2007; **67**: 7335–42.
33 Kinoshita M, McDannold N, Jolesz FA, Hynynen K. Noninvasive localized delivery of Herceptin to the mouse brain by MRI-guided focused ultrasound-induced blood–brain barrier disruption. *Proc Nat Acad Sci USA* 2006; **103**: 11 719–23.
34 Sampson JH, Crotty LE, Lee S *et al.* Unarmed, tumor-specific monoclonal antibody effectively treats brain tumors. *Proc Nat Acad Sci USA* 2000; **103**: 11 719–23.

Association of epidermal growth factor receptor (*EGFR*) gene mutations with *EGFR* amplification in advanced non-small cell lung cancer

Ryotaro Morinaga,[1,2,3] Isamu Okamoto,[1,8] Yoshihiko Fujita,[4] Tokuzo Arao,[4] Masaru Sekijima,[6] Kazuto Nishio,[4] Hiroyuki Ito,[5] Masahiro Fukuoka,[7] Jun-ichi Kadota[2] and Kazuhiko Nakagawa[1]

[1]Department of Medical Oncology, Kinki University School of Medicine, 377-2 Ohno-higashi, Osaka-Sayama, Osaka 589-8511; [2]Second Department of Internal Medicine and [3]Department of Medical Oncology, Oita University Faculty of Medicine, 1-1 Idaigaoka, Yuhu, Oita 879-5593; [4]Department of Genome Biology, [5]Department of Pathology, Kinki University School of Medicine, 377-2 Ohno-higashi, Osaka-Sayama, Osaka 589-8511; [6]Research Division for Advanced Technology, Kashima Laboratory, Mitsubishi Chemical Safety Institute, 14 Sunayama, Kamisu, Ibaraki 314-0255; [7]Department of Internal Medicine, Kinki University School of Medicine, Sakai Hospital, 2-7-1 Harayamadai, Minami-ku, Sakai, Osaka 590-0132, Japan

(Received May 28, 2008/Revised August 5, 2008/Accepted August 6, 2008/Online publication October 16, 2008)

Somatic mutations in the epidermal growth factor receptor (*EGFR*) gene are associated with the response to *EGFR* tyrosine kinase inhibitors in patients with non-small cell lung cancer (NSCLC). Increased *EGFR* copy number has also been associated with sensitivity to these drugs. However, given that it is often difficult to obtain sufficient amounts of tumor tissue for genetic analysis from patients with advanced NSCLC, the relationship between these two types of *EGFR* alterations has remained unclear. We have now evaluated *EGFR* mutation status both by direct sequencing and with a high-sensitivity assay, the Scorpion-amplification-refractory mutation system, and have determined *EGFR* copy number by fluorescence *in situ* hybridization (FISH) analysis in paired tumor specimens obtained from 100 consecutive patients with advanced NSCLC treated with chemotherapy. *EGFR* mutations or FISH positivity (*EGFR* amplification or high polysomy) were apparent in 18% (18/100) and 32% (32/100) of patients, respectively. The Scorpion-amplification-refractory mutation system was more sensitive than direct sequencing for the detection of *EGFR* mutations. Furthermore, *EGFR* mutations were associated with *EGFR* amplification ($P = 0.009$) but not with FISH positivity ($P = 0.266$). Our results therefore suggest the existence of a significant association between *EGFR* mutation and *EGFR* amplification in patients with advanced NSCLC. (*Cancer Sci* 2008; 99: 2455–2460)

The epidermal growth factor receptor (EGFR) is a receptor tyrosine kinase of the ErbB family and has been implicated in the proliferation and survival of cancer cells. Aberrant expression of *EGFR* has been detected in many human epithelial malignancies, including non-small cell lung cancer (NSCLC).[1,2] This receptor has therefore been identified as a promising target for anticancer therapy, and several agents have been synthesized that inhibit its tyrosine kinase activity. *EGFR* tyrosine kinase inhibitors (TKI) have been evaluated most extensively in individuals with NSCLC, and they have had a substantial impact on the treatment of this disease by offering additional therapeutic options for patients with advanced NSCLC.[3–6]

Somatic mutations in the tyrosine kinase domain of *EGFR* have been detected in a subset of NSCLC patients who respond to EGFR TKI[7–9] and have been shown to be closely associated with sensitivity to these drugs.[10–14] Indeed, we and others have prospectively demonstrated a high response rate to EGFR TKI therapy in NSCLC patients with *EGFR* mutations.[15–21] An increased copy number of the *EGFR* gene, as revealed by fluorescence *in situ* hybridization (FISH), has also emerged as an effective molecular marker of EGFR TKI sensitivity in NSCLC.[22–24] We previously showed that *EGFR* mutation and *EGFR* amplification are associated in human NSCLC cell lines and that endogenous EGFR expressed in such cell lines positive for both of these *EGFR* alterations are activated constitutively.[25] However, the relationship between *EGFR* mutation and FISH positivity for *EGFR*, which reflects gene amplification or high polysomy, has remained unclear.[22–24,26,27] Indeed, only a few studies have evaluated the relationship between mutation and gene copy number for *EGFR* because of the difficulty in obtaining tumor samples suitable for genetic analysis from individuals with advanced NSCLC. We previously showed that the Scorpion-amplification-refractory mutation system (ARMS) is a sensitive technique for the detection of *EGFR* mutations in tumor specimens such as pleural effusion fluid or tissue obtained by transbronchial needle aspiration.[28–30] In the present study, we evaluated *EGFR* mutation status in small tumor specimens from patients with advanced NSCLC both by direct sequencing and by Scorpion-ARMS and compared the sensitivity of these methods for the detection of *EGFR* mutations. Furthermore, we determined *EGFR* copy number by FISH analysis in paired tumor specimens and examined its relationship to *EGFR* mutation.

Materials and Methods

Patients. The present retrospective study recruited consecutive patients with advanced NSCLC who received chemotherapy at Kinki University Hospital between January 2003 and December 2005. Patients eligible for the study had histologically confirmed stage III or IV NSCLC that was not curable by surgical resection or radiotherapy, irrespective of the presence of measurable lesions or good performance status (PS). Patients with recurrence after surgical resection were excluded. Complete clinical information and tissue blocks suitable for genetic analysis were available for 100 patients. We examined the relationship between *EGFR* mutation and *EGFR* copy number as well as the influence of these *EGFR* alterations on clinical outcome. Tumor response was assessed by computed tomography and evaluated according to the Response Evaluation Criteria in Solid Tumors.[31] Survival was calculated from the date of initiation of chemotherapy either to the date of death from any cause or to the date of last contact. Some patients had been receiving EGFR TKI treatment before the demonstration in 2004 that mutations in *EGFR* confer increased sensitivity to these drugs. Moreover, many patients had already died before the initiation of our genetic analysis, preventing us from obtaining informed consent. The institutional review board

[8]To whom correspondence should be addressed.
E-mail: chi-okamoto@dotd.med.kindai.ac.jp

doi: 10.1111/j.1349-7006.2008.00962.x

therefore approved our study protocol with the conditions that samples would be processed anonymously and analyzed only for somatic mutations (not for germline mutations) and that the study would be disclosed publicly, according to the Ethical Guidelines for Human Genome Research published by the Ministry of Education, Culture, Sports, Science, and Technology, the Ministry of Health, Labor, and Welfare, and the Ministry of Economy, Trade, and Industry of Japan. The present study also conforms to the provisions of the Declaration of Helsinki.

Identification of *EGFR* mutations. The tumor specimens were fixed with formalin and embedded in paraffin. DNA was extracted with the use of a QIAamp Micro kit (Qiagen K.K., Tokyo, Japan) from tumor tissue derived either by macrodissection or by laser-capture microdissection carried out to enrich tumor cells. Polymerase chain reaction-based direct sequencing of exons 18–21 and ARMS with designed 'Scorpion' primers were applied for the allele-specific detection of *EGFR* mutations. Only the following previously described mutations[7,8] were classified as mutations in the present study: G719X in exon 18, deletion of E746 to A750 or of neighboring residues in exon 19, as well as L858R and L861Q in exon 21. Patients were regarded as *EGFR* mutation positive if a mutation in *EGFR* was detected either by direct sequencing or by ARMS. All mutations were confirmed by analysis of at least two independent amplification products.

Determination of *EGFR* copy number. *EGFR* copy number was determined by FISH analysis with the use of dual-color DNA probes (LSI *EGFR* SpectrumOrange/CEP 7 SpectrumGreen; Vysis, Downers Grove, IL, USA). The tumor specimens were classified into six categories on the basis of the FISH results, as described previously.[22] Those with high polysomy (≥4 copies of *EGFR* in ≥40% of cells) or gene amplification (presence of a tight *EGFR* gene cluster and a ratio of *EGFR* to chromosome 7 of ≥2 or ≥15 copies of *EGFR* per cell in ≥10% of cells analyzed) were considered FISH positive, with those in the remaining categories being considered FISH negative.

Statistical analysis. The relationships among *EGFR* status, clinical characteristics, and tumor response to EGFR TKI were analyzed with Fisher's exact test as appropriate. Survival curves were constructed by the Kaplan–Meier method, and the differences in survival between patient subgroups were compared by the log-rank test. The impact of various factors on survival was evaluated by univariate and multivariate analysis according to the Cox regression model. A P-value <0.05 was considered statistically significant. All statistical analysis was carried out with StatView software (SAS Institute, Cary, NC, USA).

Results

Patient characteristics. Between January 2003 and December 2005, a total of 125 consecutive patients diagnosed histologically with advanced NSCLC underwent chemotherapy at Kinki University Hospital. Tissue specimens from 100 patients were assessable for both *EGFR* mutation and *EGFR* copy number. Of these specimens, 72 were obtained by bronchoscopic biopsy, 15 by percutaneous needle biopsy (12 from lung, two from bone, and one from lymph node), six by thoracoscopic biopsy, and seven by surgery for diagnosis or palliative therapy. The clinical characteristics of these 100 patients are shown in Table 1. Most of the patients were male (64%) and had a history of smoking (67%), and adenocarcinoma was the most prevalent tumor histology (61%). Most patients (83%) also had a good Eastern Cooperative Oncology Group PS (0 or 1), and 63% received second-line or subsequent rounds of chemotherapy. Fifty-three patients (53%) were treated with EGFR TKI. Seventy patients (70%) had died by the time of genetic analysis, with the median follow-up time for the 30 survivors being 14.6 months.

***EGFR* alterations in non-small cell lung cancer.** Patients were analyzed for *EGFR* mutations by direct sequencing of exons 18 through 21 and by Scorpion-ARMS (Table 2). *EGFR* mutations, consisting of in-frame deletions in exon 19 ($n = 5$) and point mutations in exon 21 ($n = 13$), were detected in 18 patients (18%). Eight *EGFR* mutations were detected by direct sequencing and 16 mutations were detected by Scorpion-ARMS. Ten of the 16 mutations detected by Scorpion-ARMS were not identified by direct sequencing. However, two of the deletions in exon 19 (E746_S752 and E746_T751) that were detected by direct sequencing were not identified by Scorpion-ARMS, given that the Scorpion primers were designed only for detection of the E746_A750 deletion in exon 19. *EGFR* mutations were significantly more frequent in tumors of women than in those of men (33 vs 9%), in adenocarcinomas than in tumors with other histologies (28 vs 3%), and in never-smokers than in smokers (42 vs 6%) (Fig. 1a). One of the 18 *EGFR* mutations was detected in a squamous cell carcinoma. Determination of *EGFR* copy number by FISH analysis revealed gene amplification in six patients and high polysomy in 26 patients, with 32 patients thus being classified as FISH positive (Table 3). In contrast to *EGFR* mutation, FISH

Table 1. Characteristics of patients with advanced non-small cell lung cancer ($n = 100$)

Characteristic	Subset	No. patients
Sex	Male	64
	Female	36
Smoking history	Never-smoker	33
	Smoker	67
Tumor histology	Adenocarcinoma	61
	Other	39
Eastern Cooperative Oncology Group performance status	0	24
	1	59
	≥2	17
No. chemotherapies	1	37
	≥2	63

Table 2. Detection of epidermal growth factor receptor (*EGFR*) mutations by direct sequencing or amplification-refractory mutation system (ARMS) ($n = 100$)

Site	Mutation	Direct sequencing	ARMS	Direct sequencing or ARMS
Exon 19	15-bp deletion	1	3	3
	16-bp deletion	1	0	1
	19-bp deletion	1	0	1
Exon 21	L858R	5	13	13
Total		8 (8%)	16 (16%)	18 (18%)

Table 3. Determination of epidermal growth factor receptor gene copy number by fluorescence *in situ* hybridization (FISH) analysis ($n = 100$)

FISH status	Finding	No. patients
Positive	Gene amplification	6
	High polysomy	26
	Total	32
Negative	Low polysomy	35
	High trisomy	2
	Low trisomy	26
	Disomy	5
	Total	68

doi: 10.1111/j.1349-7006.2008.00962.x